# FREQUENCY PULLING OF THE VAN DER POL OSCILLATOR

# FREQUENCY PULLING OF THE VAN DER POL OSCILLATOR

by

IAN HUGH OUTRAM

A Thesis

Submitted to the Faculty of Graduate Studies

in Partial Fulfilment of the Requirements

for the Degree

Master of Engineering

McMaster University

May 1967

MASTER OF ENGINEERING (1967) McMaster University
(Electrical Engineering) Hamilton, Ontario

TITLE: Frequency Pulling of the van der Pol Oscillator

AUTHOR: Ian Hugh Outram

SUPERVISOR: Professor A. S. Gladwin

NUMBER OF PAGES: viii, 74

SCOPE AND CONTENTS:

The pulling of the free frequency of a nonlinear saturation-type oscillator by an external forcing signal is investigated, the oscillator being described by the van der Pol equation.

Both experimental and theoretical methods are used to find the relation between the amplitude and frequency of the external signal and the frequency pulling of the oscillator.

The case of a sinusoidal forcing signal is examined theoretically, and experimental results are shown for a sinusoidal signal and also for narrow band noise.

ABSTRACT

The frequency pulling of the van der Pol nonlinear oscillator due to an external forcing signal is investigated. The nonlinearity is of the zero-memory symmetric-cut-off type following a cube law.

An experimental oscillator was built, and curves of the frequency shift of the oscillator fundamental against the magnitude of the input forcing signal are shown, both for a sinusoidal input and for a narrow band noise input. An empirical result is derived.

The case of the sinusoidal input is examined theoretically. The importance of harmonic and intermodulation frequencies in the oscillator output is shown, and relations giving the oscillator frequency shift are given for small forcing amplitudes and for large amplitudes when the oscillator is nearly synchronized.

ACKNOWLEDGEMENTS

I wish to thank Dr. A. S. Gladwin for many useful discussions and helpful guidance during the course of this work, and also in the preparation of this thesis.

I would also like to express my appreciation of a number of useful suggestions from Dr. R. Kitai and Dr. N. K. Sinha.

Acknowledgement is also made for the generous financial support of the National Research Council under grant A902.

Also finally, I would like to thank Miss M. Kaneary for typing this thesis.

TABLE OF CONTENTS


| | | PAGE |
|---|---|---|
| CHAPTER 1 - | INTRODUCTION | 1 |
| 1.1 | Review of the Literature | 3 |
| CHAPTER 2 - | THE VAN DER POL OSCILLATOR | 7 |
| 2.1 | Oscillation Equation | 7 |
| 2.2 | Solution of the van der Pol Equation | 9 |
| CHAPTER 3 - | FREQUENCY PULLING OF THE VAN DER POL OSCILLATOR | 10 |
| 3.1 | The Approach of A. W. Gillies | 11 |
| 3.2 | Variational Approach | 18 |
| | 3.2-1 The variational equation | 18 |
| | 3.2-2 Frequency of the free oscillation at the stability limit | 21 |
| | 3.2-3 Frequency of the free oscillation for small disturbances | 25 |
| 3.3 | Elementary Approach for a large Narrow Band Noise Input | 30 |
| 3.4 | Discussion of the Methods | 32 |
| CHAPTER 4 - | EXPERIMENTAL INVESTIGATION | 37 |
| 4.1 | Oscillator Circuit | 37 |
| 4.2 | Noise Source | 39 |
| 4.3 | Input/Output Circuits | 40 |

| | | PAGE |
|---|---|---|
| 4.4 | Measurement of Circuit Parameters | 41 |
| 4.5 | Experimental Technique | 44 |
| 4.6 | Experimental Results | 45 |
| 4.7 | An Empirical Result | 45 |
| 4.8 | Accuracy | 52 |
| CHAPTER 5 - | CONCLUSIONS | 54 |
| APPENDICES: | | |
| A - | THE METHOD OF VAN DER POL | 55 |
| B - | FREQUENCY COMPARISON | 61 |
| C - | COMPUTER ANALYSIS | 63 |
| D - | APPARATUS | 71 |
| REFERENCES | | 72 |

TABLE OF ILLUSTRATIONS


| FIGURE | | PAGE |
|---|---|---|
| 2.1 | van der Pol Oscillator Equivalent Circuit | 7 |
| 2.2 | Nonlinear Element Voltage/Current Characteristic | 7 |
| 3.1 | Frequency Shift Calculated from Gillies' Method | 17 |
| 3.2 | Relative Amplitudes of the Harmonics of the Forced Oscillator near Locking | 21 |
| 4.1 | Circuit Diagram of the Experimental Oscillator | 38 |
| 4.2 | Circuit Diagram of the Filter used to Obtain Narrow Band Noise | 40 |
| 4.3 | Geometric Analysis of the Nonlinear Element Characteristic | 41 |
| 4.4 | Experimental Waveforms<br>(a) Voltage and Current Waveforms for the Nonlinear Element<br>(b) Voltage/Current Characteristic for (a)<br>(c) Output Waveform of the Forced Oscillator | 46 |
| 4.5 | Frequency Shift vs Input Current (Narrow Band Noise Input) for Input Frequencies Less Than $\omega_o$ | 47 |
| 4.6 | Frequency Shift vs Input Current (Narrow Band Noise Input) for Input Frequencies Greater Than $\omega_o$ | 48 |
| 4.7 | Frequency Shift vs Input Current (Sinusoidal) | 49 |

| FIGURE | | PAGE |
|---|---|---|
| 4.8 | Frequency Shift vs Input Current (Sinusoidal), Log-Log Plot | 51 |
| A1 | Resonance Curves for the van der Pol Oscillator | 57 |
| A2 | Locking Current vs Frequency for the van der Pol Oscillator | 60 |
| B1 | Block Diagram of the Circuit Used for Frequency Comparison | 61 |
| B2 | Lissajou Figure Obtained When the y Plate Frequency is the Same as a Component of the x Plate Signal | 61 |
| C1 | van der Pol Oscillator Starting Transient | 65 |
| C2 | Waveform of the Forced van der Pol Oscillator | 66 |


**********

COMPUTER PROGRAMMES


| PROGRAMME | | PAGE |
|---|---|---|
| 1 | MIMIC Source-Language Programme for the van der Pol Oscillator | 67 |
| 2 | MIDAS Source-Language Programme as for (1) | 67 |
| 3 | Fourier Harmonic Analysis of the Oscillator Output Obtained from Programme 1. | 68 |


**********

# CHAPTER I

# INTRODUCTION

Nonlinear systems exhibit phenomena not found in linear systems. For example, a spring-mass system with a nonlinear spring will have resonance curves similar to the linear case, but skewed over, and the amplitude may have discontinuous jumps as the frequency is varied.

In the autonomous case, an oscillator may have nonlinear damping. The basic negative resistance oscillator is made up of an antiresonant circuit in parallel with a negative resistance to cancel losses, and follows the (normalized) equation $\frac{d^2e}{dt^2} + e = 0$ where e is the output voltage. The frequency is 1 and the amplitude is entirely determined by the initial conditions. In the more realistic case, the negative resistance element is not precisely linear, due to the curvature in the tube or transistor characteristic for example. The van der Pol[1] equation

$$\frac{d^2e}{dt^2} - \alpha (1 - e^2) \frac{de}{dt} + e = 0 \qquad (1)$$

describes an oscillating system where the damping is negative near the origin, but becomes positive away from it. If $\alpha$ is zero, the system is linear, but if $\alpha$ is finite, however small, then the system has a fixed amplitude, the frequency is slightly less than 1, and harmonics appear at the output. The principal of superposition does not apply, and special analytical techniques have to be used. First order approximate solutions

to the van der Pol equation may be found in the standart texts. A number of methods of solution may be used, for example, the principle of harmonic balance[2], the perturbation method[3], the method of Andronov and Witt[4], or van der Pol method[1, 5].

If an external forcing term F(t) is introduced on the right hand side of equation (1), then both the frequency and amplitude are changed from the freely oscillating case. If F(t) is sinusoidal, the free oscillation frequency is pulled towards the frequency of F(t), and modulation product frequencies appear at the output.

The response of the forced van der Pol oscillator has attracted some attention, both in the case of F(t) a stochastic function[6 - 11], and a deterministic one[1,3,12,13,14,16].

If the oscillator is used as a local frequency standard, then the effect of any extraneous inputs on the monochromacity or on the mean frequency is of great importance. This work is concerned with the deviation of the oscillator frequency from its unperturbed value for inputs F(t) of small amplitude, and for small $\alpha$.

For the experimental investigation an oscillator was built which corresponded closely to the ideal van der Pol oscillator. To investigate the effect of random noise on the oscillator quantitatively, white noise from a noise generator was passed through a band-pass filter, and the resultant narrow band noise injected into the oscillator through a buffer amplifier. Internal noise, such as shot or flicker noise, can then be neglected in comparison with the injected noise, and quantitative measurements made[15].

Chapter 2 describes the general nonlinear oscillator, and the van der Pol equation which describes an oscillator with cubic nonlinearity is derived.

Chapter 3 details the theoretical methods used to investigate the frequency pulling phenomenon. Two main methods are used, the general method of Gillies[12a] and a novel variational method, both of which demonstrate the importance of modulation products between the free and forced oscillations. A qualitative explanation of the oscillator behaviour under the influence of large amplitude narrow band noise is also given.

Chapter 4 gives details of the experimental methods used.

## 1.1 Review of the Literature:

There is considerable literature concerned with the problem of noise in non-linear oscillators. In 1956, in the case of δ-correlated white noise Rytov[10] used correlation methods to deduce expressions for the amplitude and phase fluctuations of the oscillator output. The part of the noise spectrum near the oscillator frequency is considered to be the major influence, and is expressed as a sine wave of slowly varying amplitude and phase. The method uses Fourier series and power series expansions to obtain a series of approximate linear equations. A simplification is made by associating the forcing term with $\alpha^2$. A description of the method is given by Tang[10b].

In 1957 Garstens[17] investigated the power spectrum of the noise driven oscillator by separating the nonlinear part of the noise from the linear part, and calculating the two spectral densities. The correlation

between the two parts is, however, not calculated.

Edson[7] deals statistically with starting time jitter and found that it depended only on "a", the value of the nonlinear negative resistance of the origin. The phase and amplitude spectral densities are calculated for a driving force of narrow band noise centered about the oscillator frequency, and show that the oscillator spectral line width is broadened (phase modulation spectrum) and superimposed on weak broadband noise (amplitude modulation spectrum). The paper deals with a general nonlinearity. The parameter describing the nonlinearity is not unique but depends on the magnitude of the disturbance as well as the values of the circuit elements, and so may not be easy to evaluate for the practical case.

Mullen[18] calculates the spectrum of the noise perturbed van der Pol oscillator, and obtains an approximate result by neglecting harmonics and modulation products. Golay[9] considers monochromacity in an A.G.C. oscillator.

More recently, Hafner[11] used a different approach, not involving any linearization of the non-linear equation, unlike previous work, or the slowly varying principle[11b], where a solution of the form $e = R \cos(\omega_o t - \theta)$ is assumed and R and $\theta$ are slowly varying quantities compared to $\omega_o t$, where $\omega_o$ is the approximate oscillator frequency. The only assumption is that (in the derivation of the perturbation equation) $u^2$ and $u\dot{u}$, where u is the disturbance, are negligably small compared to u. The van der Pol nonlinearity is taken as a specific example, and a perturbation equation, linear in the (small) disturbance is obtained. This equation is similar to the variational equation used later in this work.

However, although harmonics are considered, intermodulation products are not, the output being considered as narrow band noise at the oscillator frequency.

It can be seen that considerable progress has been made with white noise, or narrow band noise centered about the oscillator frequency, as the forcing function. If the disturbance is at a different frequency from the free running frequency, intermodulation terms are formed at frequencies away from the harmonics of the fundamental and these are responsible for the frequency pulling of the free oscillator frequency[12b] in the same way that the harmonics of the fundamental cause a slight deviation of the free oscillation frequency from that of the resonant circuit in the unperturbed oscillator.

There are a number of papers using the Sine Wave model, in which the disturbance is approximated by a sine wave. As pointed out by Edson[7], this is not a very realistic model of noise, as the effects of fluctuating phase and amplitude are omitted completely. It does, however, permit an investigation of frequency pulling phenomena.

A general approach using a sinusoidal forcing function is given by Adler[20], for a nonlinear oscillator, or a linear A.G.C. oscillator whose A.G.C. time constant is much less than the beat frequency between the free and forced oscillations. Stover[21], extending Adler's analysis, examines the output spectrum. His results are verified by Raue and Ishii[13], but only qualitative experimental agreement was found with the theoretical values of the frequency and amplitude of the fundamental component.

A different technique is used by Gillies[12a]. Here, power and Fourier series are used to reduce the problem to a single equation which may be solved for the frequency and amplitude of the fundamental. In theory the method may be carried to any desired accuracy, but in practice the algebra becomes very tedious after the fifth order modulation terms are taken into account. Only qualitative agreement with experiment was obtained when the method was used to examine frequency pulling in the van der Pol oscillator (Chapter 3).

CHAPTER II

THE VAN DER POL OSCILLATOR

## 2.1 Oscillation Equation:

The oscillator circuit used consisted of an LC parallel circuit in parallel with a cube-law voltage controlled resistor as in Figures 2.1 and 2.2 below.

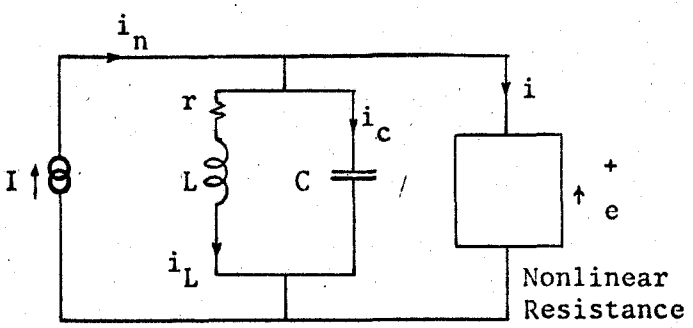


FIGURE 2.1

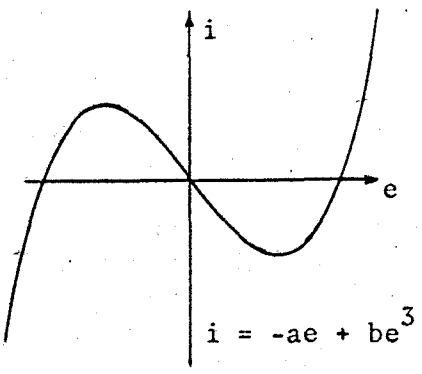


Nonlinear Resistance Characteristic

FIGURE 2.2

It can be seen that

$$i_n = i_L + i_C + i$$

where

$$i = -ae + be^3 \qquad i_C = C\frac{de}{dt}$$

$$e = ri_L + L\frac{di_L}{dt} \qquad i_n = I\cos(\omega_1 t + \phi)$$

Hence,

$$I\cos(\omega_1 t + \phi) = C\frac{de}{dt} - ae + be^3 + \frac{1}{L}\int e\,dt + \frac{r}{L}\int (i_C + i - i_n)\,dt$$

Differentiating:

$$\ddot{e} - \frac{a}{C}\dot{e} + \frac{3b}{C}e^2\dot{e} + \frac{1}{LC}e + \frac{r}{LC}\left[C\dot{e} - ae + be^3 - I\omega_1 \cos(\omega_1 t + \phi)\right] = -\frac{I\omega_1}{C}\sin(\omega_1 t + \phi)$$

In general the Q of the tuned circuit is high and so the term in r can be neglected. Hence,

$$\ddot{e} - \frac{a}{C}\left(1 - \frac{3b}{a}e^2\right)\dot{e} + \frac{1}{LC}e = -\frac{I\omega_1}{C}\sin(\omega_1 t + \phi)$$

or

$$\ddot{e} - \alpha(1 - \beta e^2)\omega_o\dot{e} + \omega_o^2 e = -\frac{I\omega_1}{C}\sin(\omega_1 t + \phi) \qquad (2)$$

where

$$\alpha = \frac{a}{C\omega_o} \qquad \beta = \frac{3b}{a} \qquad \omega_o^2 = \frac{1}{LC}$$

which is the Van der Pol Equation, with a forcing term.

If there is a positive resistance R shunting the circuit (the internal resistance of the current source, for example), then the value of a is modified.

$$a \rightarrow \left(a - \frac{1}{R}\right)$$

$\beta$ is a factor which normalizes the amplitude. By replacing e by $\frac{e}{\sqrt{\beta}}$ and t by $\frac{t}{\omega_o}$, the van der Pol equation in its normalized form is obtained, Equation (1), for the unforced case.

## 2.2 Solution of the van der Pol Equation:

The van der Pol equation may be solved using standard techniques[1,2,3,4,5]. Since these methods are well known, only the results will be quoted here.

The unperturbed oscillator output is:

$$e = (2 - \frac{1}{8}\alpha^2) \cos \omega t + \frac{3}{4} \alpha \sin \omega t + \frac{3}{16} \alpha^2 \cos 3 \omega t - \frac{1}{4} \alpha \sin 3\omega t$$

$$- \frac{5}{96} \alpha^2 \cos 5 \omega t + - - - -$$

where the frequency is given by

$$\omega = (1 - \frac{\alpha^2}{16} ----)$$

for the normalized van der Pol equation (1).

Thus it can be seen that the effect of the nonlinearity is to fix the amplitude of the output, and decrease the frequency.

The above solutions are valid only if the nonlinearity is small (i.e. $\alpha << 1$). If this is not so, the output is not approximately sinusoidal as above, but consists of a relaxation type of oscillation[24].

The method used by van der Pol for the driven oscillator is given in Appendix A. The oscillator resonance curves, and the synchronization limits are derived.

The output in the region of combination oscillations (of free and forced frequencies) has been calculated to the first order terms, using the above methods, and the result is also given.

# CHAPTER 3

## FREQUENCY PULLING OF THE VAN DER POL OSCILLATOR

If an external signal is introduced into a linear oscillator, the output is merely the sum of the oscillator output and the external signal. In the case of the nonlinear van der Pol type of oscillator, this is not so. Both the frequency and amplitude of the free oscillation are affected, and if the external signal is too large, the free oscillation will be suppressed and the forced oscillation alone will exist, and the oscillator is said to be synchronized or entrained.

As the injected signal increases in magnitude from zero, the free oscillation decreases in amplitude and the frequency is pulled towards that of the injected driving signal, until the free oscillation is suppressed. Simultaneously, sidebands appear about the free frequency, of spacing equal to the frequency difference between the driver and partially pulled oscillator frequencies. The presence of these sidebands was observed in the experimental oscillator built, and has been observed in other types of oscillator, such as a reflex klystron[13], a tunnel diode oscillator[21], and a bulk GaAs oscillator[25].

In paragraph 3.2 the method of A. W. Gillies[12a] is used to calculate the amplitude and frequency of the free oscillation in the driven van der Pol oscillator. The results are found to be in only qualitative agreement with experiment.

In paragraph 3.3 a variational approach is used to find the free oscillation frequency just before the oscillator becomes entrained.

Although a sine wave is not a realistic model of narrow band noise, the frequency pulling of each is similar (see Figures 4.5 and 4.6 ) in the region where synchronization does not occur, and both follow a square law (see Paragraph 4.7).

3.1 The Approach of A. W. Gillies:

The method is to assume a solution v which contains the fundamental frequencies (free and forced) and their higher harmonics and intermodulation products. This is substituted into the van der Pol equation and the coefficient of the component of the free frequency equated to zero by the principle of harmonic balance. This component consists of the fundamental term, and terms resulting from the intermodulation of the higher order terms. This then yields a complex equation describing the frequency and amplitude of the fundamental, from which the deviation of the free frequency from its free running value can be found.

It is assumed that

$$\omega_a \neq \frac{n}{m} \omega_b$$

where $\omega_a$ is the free frequency

$\omega_b$ is the forcing frequency

and m, n are integers. That is, no combination of $\omega_a$ and $\omega_b$ is near $\omega_a$.

The basic approach of considering the oscillator output as the sum of the forced and fundamental frequencies and their modulation products and harmonics is described by Gillies[12b]. The complete analysis of the effect of these frequencies on the mean oscillator free frequency is given in his earlier paper[12a]

Consider the driven van der Pol equation(2), integrated and written in the form

$$-\frac{I}{C}\cos\omega_b t = (\alpha\omega_o - D - \frac{\omega_o^2}{D})\, v - \frac{1}{3}\alpha\beta\omega_o\, v^3 \qquad (3)$$

where D is the differential operator, v is the oscillator output and e is the external driving input. The notation of e, v, $\omega_a$, $\omega_b$ is used in this section to conform with Gillies paper[12a]. Then equation (3) is of the form

$$Ye = (Y + P_1)\, v + P_3\, v^3$$

If a steady state has been reached when v is of the form

$$\sum_k V_{\omega_k} e^{j\omega_k t} + V_{-\omega_k} e^{-j\omega_k t}$$

then D may be replaced by $j\omega$, and hence

$$Ye = -\frac{I}{C}\cos\omega_b t, Y + P_1 = \alpha\omega_o - j(\omega - \frac{\omega_o^2}{\omega}),\ P_3 = -\frac{\alpha\beta\omega_o}{3} \qquad (4a)$$

(Expressed in terms of Figure (2.1),

$Y = -\frac{y}{C}$ where y is the admittance of the LC tank circuit

$P_1 = \frac{a}{C}$ $\quad P_3 = -\frac{b}{C}$

$e = \frac{I}{y}\cos\omega_b t$, the equivalent voltage generator in series with the tank circuit.)

In the general case where the nonlinearity is not just a cubic (Fig. 2.2), but a general polynomial, then equation (4) takes the form

$$Ye = (Y + P_1)\, v + P_2 v^2 + P_3 v^3 + \text{-----}$$

The output v consists of the sum of the two first-order (free and

forced) frequencies together with higher order modulation frequencies $\omega_a + \omega_b$, $\omega_a - \omega_b$, $2\omega_a$, $2\omega_b$ being the second order terms, $3\omega_a$, $3\omega_b$, $\omega_a + \omega_b + \omega_a$, $\omega_a + \omega_b - \omega_a$, ---, being the third order terms, and so on for the higher order terms, where $\omega_a$ is the frequency of the free oscillation.

Hence let

$$v = V^{(1)} + V^{(2)} + V^{(3)} + \text{-----} \tag{6}$$

where $V^{(n)}$ represents the sum of the $n^{th}$ order modulation products. Subtitution of this into equation ( 5 ) yields:

$$\begin{aligned} Ye = (Y + P_1)\ [\ V^{(1)} + V^{(2)} + V^{(3)} + \text{----}\ ] \\ + P_2\ [\ V^{(1)} + V^{(2)} + V^{(3)} + \text{----}\ ]^2 \\ + P_3\ [\ V^{(1)} + V^{(2)} + V^{(3)} + \text{----}\ ]^3 \end{aligned} \tag{7}$$

Terms of like order can now be equated to give a set of recursive equations for determining the $V^{(n)}$:

$$Ye = (Y + P_1)\ V^{(1)} \tag{8a}$$

$$0 = (Y + P_1)\ V^{(2)} + P_2 V^{(1)2} \tag{8b}$$

$$0 = (Y + P_1)\ V^{(3)} + 2P_2 V^{(1)} V^{(2)} + P_3 V^{(1)3} \tag{8c}$$

The $V^{(n)}$ can be expanded into their frequencies. For the synchronized oscillator these are:

$$V^{(1)} = V_b^{(1)} + V_{-b}^{(1)} \tag{9a}$$

$$V^{(2)} = V_{2b}^{(2)} + V_o^{(2)} + V_{-2b}^{(2)} \tag{9b}$$

$$V^{(3)} = V_{3b}^{(3)} + V_b^{(3)} + V_{-b}^{(3)} + V_{-3b}^{(3)} \tag{9c}$$

where

$$V_b^{(1)} = (|V_b^{(1)}|\ \underline{/\phi_b^{(1)}})\ e^{j\omega_o t}$$

If both free ($\omega_a$) and forced ($\omega_b$) oscillations are present, then

$$V^{(1)} = V_a^{(1)} + V_{-a}^{(1)} + V_b^{(1)} + V_{-b}^{(1)} \qquad (10)$$

and hence $V^{(n)}$ $n = 2, 3, \ldots$ can be found in terms of $V_a^{(1)}$, $V_{-a}^{(1)}$, $V_b^{(1)}$, $V_{-b}^{(1)}$ from equations (8a, 8b,.....), and equation (9) will thus contain cross modulation terms as well. [The first order equation (8a) yields $\omega_a = \omega_o$ (1 p76, 2 p215), and equations (8b, 8c,...) will contain terms of frequency $\omega_a$. The procedure is hence modified by letting $V_a^{(1)}$ be the resultant term in $\omega_a$, and setting the higher order terms in $\omega_a$ in equations (8) to zero. Equation (7) is then used instead of equation (8a)]

The $V^{(n)}$ can now be found from equation (10) and equations (8b, 8c,), and substituted back into equation (7). In this way, equation (7) is identically satisfied for all frequencies except the fundamental. The fundamental terms can now be picked out and equated to zero, the left hand side of equation (7) having no fundamental ($\omega_a$) term.

Equation (7) is then a complex equation determining the frequency and amplitude of the fundamental. The algebra is somewhat tedious, but the frequency/amplitude equation reduces, for the van der Pol oscillator (that is, $P_2 = P_4 = P_5 = P_6 = \cdots = 0$) up to the fifth order terms, to

$$0 = (Y_a + P_1) + P_3\{3V_a^2 + 6V_b^2 - 3P_3[V_a^4 \zeta_{3a} + 3V_b^4(\zeta_{a-2b} + \zeta_{a+2b}) + 12V_a^2V_b^2(\zeta_{-b} + \zeta_b) + 6V_b^4(\zeta_b + \zeta_{-b}) + 6V_a^2V_b^2(\zeta_{2a+b} + \zeta_{2a-b})]\} + OV^6 \qquad (11)$$

where $\zeta_i = \frac{1}{Y_i + P_1}$, and the superscript $^{(1)}$ has been droped from the $V^{(1)}$ for convenience. The term $V_a^{(1)} e^{j\omega_a t}$ has been cancelled throughout, and $V_b^2 = V_b^{(1)} V_{-b}^{(1)} e^{j\omega_b t} e^{-j\omega_b t}$.

The seventh order terms are numerous, but all involve products of $\zeta$, and so may be neglected in comparison with the fifth order terms. The terms in $\zeta_{3a}, \zeta_{2a+b}$ may also be neglected as being small as these frequencies are far removed from the resonant frequency

For convenience the following substitutions are now made:

$$\omega = \omega_o + \Delta\omega = \text{fundamental frequency}$$

$$\omega_1 = \omega_o + \Delta\omega_1 = \text{forcing frequency}$$

$$x = 2\Delta\omega/\alpha\omega_o$$

$$x_1 = 2\Delta\omega_1/\alpha\omega_o$$

$$y = |V_a|^2 \beta$$

$$y_1 = |V_b|^2 \beta$$

Hence, using equation ( 4 ),

$$Y_a + P_1 = \alpha\omega_o(1 - jx)$$

$$Y_{2a-b} + P_1 = \alpha\omega_o \left[1 - j\left(2x - x_1 - \frac{\alpha(x - \frac{x}{2})^2}{1 + \alpha(x - \frac{x}{2})}\right)\right] \qquad (12)$$

$$Y_{2b-a} + P_1 = \alpha\omega_o \left[1 - j\left(2x_1 - x - \frac{\alpha(x_1 - \frac{x}{2})^2}{1 + \alpha(x_1 - \frac{x}{2})}\right)\right]$$

If we neglect the $\alpha^2$ terms in the above, equation (11) becomes after substitution and separation of real and imaginary parts,

$$0 = 1 - 2y_1 - y_1^2 \left[ \frac{1}{1 + (2x_1 - x)^2} + \frac{4}{1 + x_1^2} \right] + \text{----}$$

$$0 = -x - yy_1 \frac{2(2x - x_1)}{1 + (2x - x_1)^2} + y_1^2 \frac{2x_1 - x}{1 + (2x_1 - x)} + \text{----} \qquad (13)$$

where

$$y_1 = \frac{I^2\beta}{\omega_o^2 C^2} \quad \frac{1}{\alpha^2(1 + x_1^2)}$$

from equations (4a) and (8a), which is still valid for $V_b^{(1)}$.

These equations (13) were solved for x and y for various values of $x_1$ and $y_1$. Figure 3.1 shows an experimental curve of the frequency deviation of the fundamental from its free running frequency ($=\omega_o(1-\frac{\alpha^2}{16})$ from paragraph 2.2). Also plotted is the curve given by equations (13). In this case, $\Delta\omega = 0$ when $I' = 0$ and the free oscillation coincides with $\omega_o$. This is shown (curve 1) by the fact that the curve does not start at the origin, but at a value corresponding to $\omega_o \frac{\alpha^2}{16}$, which was 90.5 Hz for the experimentally tested oscillator, for which $\omega_o$ was 216 KHz.

If the $\alpha^2$ terms in equations (12) are considered, and the terms in $\zeta_{3a}$ etc. not neglected, curve 2 results. This starts at the origin, that is, the unperturbed frequency is correct, but the curve rises too steeply, and synchronization ($y = 0$) occurs too early. With forcing frequencies nearer to $\omega_o$, these disparities were even more pronounced.

In view of this it can be concluded that either the seventh order terms are important, or that the experimental oscillator was not a true van der Pol oscillator. Since it is a second order effect which is being sought, it is important that the experimental circuit conform as nearly as possible to the ideal. The presence of a small square term in the

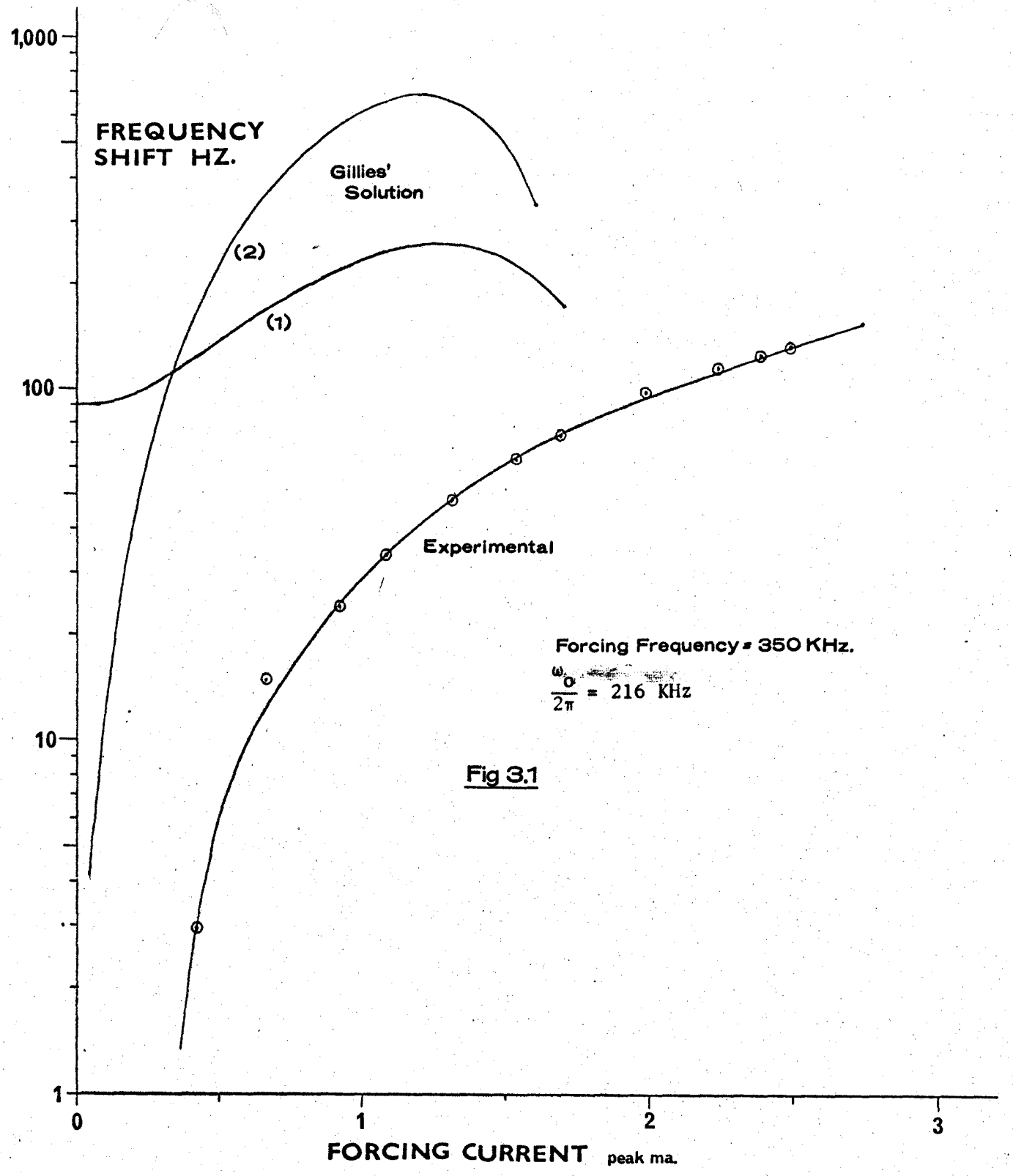
1,000
100
10
1
FREQUENCY SHIFT HZ.
Gillies' Solution
(2)
(1)
Experimental
Forcing Frequency = 350 KHz.
$\frac{\omega_o}{2\pi}$ = 216 KHz
0
1
2
3
FORCING CURRENT peak ma.

Fig 3.1

nonlinear element would cause extra spurious frequency deviations (although the second harmonic content of the oscillator output was very small (paragraph 4.1)). Also the active nonlinear element may contain some nonlinear reactance.

On the other hand, the current required to lock the oscillator agreed very well (Figure A2 ) with that calculated (Appendix A) indicating that the circuit was, to the first-order at least, a good approximation to the van der Pol circuit. However, at these higher values of the forcing current, the seventh order terms which were neglected would assume more importance, and may account for the disparities.

## 3.2 Variational Approach:

### 3.2-1 The variational equation-

The method used here is to assume a solution

$$e = e_o + \xi$$

where $e_o$ is an approximate solution and $\xi$ is a second order correction.

In the case of a general nonlinear resistance following the law

$$i = f(e)$$

the oscillator equation is

$$\ddot{e} + \frac{1}{C}\frac{df(e)}{de}\dot{e} + \omega_o^2 e = F(t) \qquad (14)$$

where $F(t) = \frac{1}{C}\frac{di_n}{dt}$

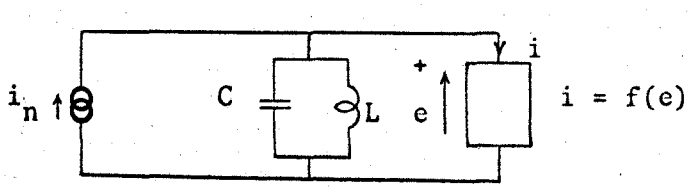

When $i = -ae + be^3$ this results in the van der Pol equation derived in Chapter 2.

This can be rewritten:

$$\frac{d^2e}{dt^2} + \frac{1}{C}\frac{df(e)}{dt} + \omega_o^2 e = F(t)$$

Let

$$e = e_o + \xi$$

$$\frac{de}{dt} = \frac{de_o}{dt} + \frac{d\xi}{dt}$$

$$\frac{d^2e}{dt^2} = \frac{d^2e_o}{dt^2} + \frac{d^2\xi}{dt^2}$$

Expanding f(e) as a Taylors series about $e_o$ gives

$$f(e) = f(e_o) + \frac{df(e_o)}{de}\xi + \frac{d^2f(e_o)}{de^2}\frac{\xi^2}{2!} + \text{------}$$

and so,

$$\frac{df(e)}{dt} = \frac{df(e_o)}{dt} + \frac{d\xi}{dt}\frac{df(e_o)}{de} + \xi\frac{d}{dt}\frac{df(e_o)}{de} + \xi\frac{d\xi}{dt}\frac{d^2f(e_o)}{de^2}$$

$$+ \frac{\xi^2}{2}\frac{d}{dt}\frac{d^2f(e_o)}{de^2} + \text{----}$$

Substituting these equations into equation (14) gives

$$\frac{d^2e_o}{dt^2} + \frac{d^2\xi}{dt^2} + \frac{1}{C}\left[\frac{df(e_o)}{dt} + \frac{d\xi}{dt}\frac{df(e_o)}{de} + \xi\frac{d}{dt}\frac{df(e_o)}{de} + \text{---}\right]$$

$$+ \omega_o^2 e_o + \omega_o^2 \xi = F(t) \qquad (15)$$

Since $e_o$ satisfies equation ( 14) to the first order, equation ( 15) reduces to the variational equation for small variations $\xi$:

$$\frac{d^2\xi}{dt^2} + \frac{1}{C}\frac{df(e_o)}{de}\frac{d\xi}{dt} + \left[\omega_o^2 + \frac{1}{C}\frac{d}{dt}\frac{df(e_o)}{de}\right]\xi = 0 \qquad (16)$$

where terms involving $\xi^2$, $\dot{\xi}\xi$, or powers of $\xi$ higher than these have been neglected.

For a system with a van der Pol nonlinearity

$$f(e_o) = i = -ae_o + be_o^3$$

$$\frac{df(e_o)}{de} = -a + 3be_o^2$$

and hence equation ( 16) becomes

$$\frac{d^2\xi}{dt^2} - \frac{1}{C}(a - 3be_o^2)\frac{d\xi}{dt} + \left[\omega_o^2 + \frac{6b}{C}e_o\frac{de_o}{dt}\right]\xi = 0$$

Writing

$$\alpha = \frac{a}{C\omega_o} \qquad \beta = \frac{3b}{a}$$

gives,

$$\frac{d^2\xi}{dt^2} - \alpha(1 - \beta e_o^2)\omega_o\frac{d\xi}{dt} + \left[\omega_o^2 + 2\alpha\beta\omega_o e_o\frac{de_o}{dt}\right]\xi = 0 \qquad (17)$$

which is the first order variational equation to the van der Pol equation (1). The stability conditions (A7) and (A8) can be derived from this equation. The oscillator output when synchronized may be written

$$e_o = E_1 \cos \omega_1 t$$

with $F(t) = -\frac{I\omega_1}{C}\sin(\omega_1 t + \phi)$.

Substituting this into equation (17) yields

$$\frac{d^2\xi}{dt^2} - \alpha\left(1 - \frac{\beta E_1^2}{2}(1 + \cos 2\omega_1 t)\right)\omega_o \frac{d\xi}{dt} + \left[\omega_o^2 - \alpha\beta\omega_o\omega_1 E_1^2 \sin 2\omega_1 t\right]\xi = 0 \qquad (18)$$

If $\xi = Ae^{st}\cos(\omega_1 t + \lambda)$ is substituted into equation (18) and terms in $e^{st}\sin\omega_1 t$ and $e^{st}\cos\omega_1 t$ separately equated to zero, two equations in A sin λ and A cos λ are formed. If the determinant of coefficients of these is then equated to zero for consistancy, a single fourth order polynomial equation in S is obtained. Applying the Routh stability condition for negative roots of S yields the stability limit equations (A7) and (A8).

### 3.2-2 Frequency of the free oscillation at the stability limit-

When the oscillator is close to the stability limit, that is, when the free oscillation has a very small amplitude and the oscillator is nearly synchronized, the output is found to consist of sidebands about the driving frequency of spacing $(\omega_1 - \omega_f)$ where $\omega_f$ is the frequency of the free oscillation. The most significant of these sidebands are those adjacent to the driving frequency, that is at $\omega_f$ and $(2\omega_1 - \omega_f)$. Using the method described in Appendix B, the approximate relative magnitudes of the sidebands are shown in Figure 3.2 below.

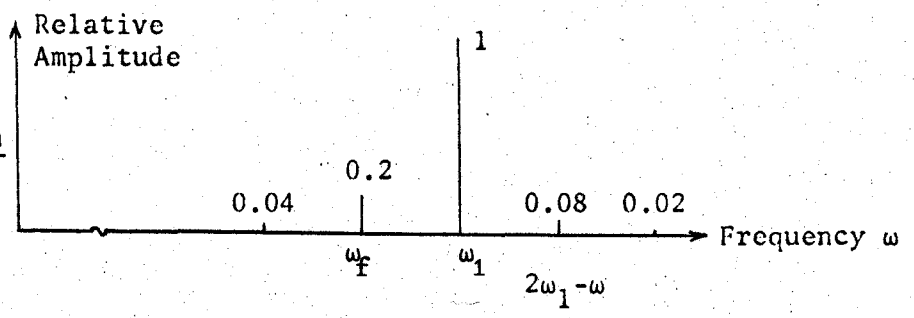


FIGURE 3.2
Output Spectrum
Near Locking

As a first approximation, therefore, let

$$\xi = A \sin (\omega_f t + \psi) + B \sin ((2\omega_1 - \omega_f)t + \theta) \tag{19}$$

and substitute this into equation (18)), together with the stability limit condition derived in Appendix A, for $\omega_1$ away from the ellipse

$$E_1^2 = \frac{2}{\beta}$$

Equating coefficients of $\sin \omega_f t$, $\cos \omega_f t$, $\sin (2\omega_1 - \omega_f)t$, $\cos (2\omega_1 - \omega_f)t$ separately to zero gives the four equations.

$$\begin{bmatrix} (\omega_o^2 - \omega_f^2) & 0 & 0 & -\alpha\omega_o \frac{\omega_f}{2} \\ 0 & (\omega_o^2 - \omega_f^2) & -\alpha\omega_o \frac{\omega_f}{2} & 0 \\ 0 & \alpha\omega_o(\omega_1 - \frac{\omega_f}{2}) & [(2\omega_1 - \omega_f)^2 - \omega_o^2] & 0 \\ \alpha\omega_o(\omega_1 - \frac{\omega_f}{2}) & 0 & 0 & [(2\omega_1 - \omega_f)^2 - \omega_o^2] \end{bmatrix}$$

$$\times \begin{bmatrix} A \cos \psi \\ A \sin \psi \\ B \cos \theta \\ B \sin \theta \end{bmatrix} = \underline{0} \tag{20}$$

The condition for consistancy is:

$$\begin{vmatrix} (\omega_o^2 - \omega_f^2) & -\alpha\omega_o \frac{\omega_f}{2} \\ \alpha\omega_o(\omega_1 - \frac{\omega_f}{2}) & [(2\omega_1 - \omega_f)^2 - \omega_o^2] \end{vmatrix} = 0$$

Substituting $\omega_f = \omega_1 - \delta$ and normalizing $\omega_o = 1$ gives:

$$\begin{vmatrix} (1 - \omega_1^2) + 2\omega_1\delta - \delta^2 & -\frac{\alpha}{2}(\omega_1 - \delta) \\ \frac{\alpha}{2}(\omega_1 + \delta) & [(\omega_1^2 - 1) + 2\omega_1\delta + \delta^2] \end{vmatrix} = 0$$

Solving this,

$$\delta = \sqrt{\omega_1^2 + 1 - \frac{\alpha^2}{8}} - \sqrt{4\omega_1^2 - \frac{\alpha^2}{4} + \frac{\alpha^4}{64}} \qquad (21)$$

Now the frequency shift of the free oscillation from its unperturbed value is

$$\omega_f - \omega_{fo} = \omega_1 - \delta - \omega_{fo}$$

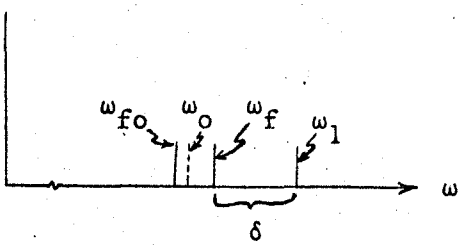


where

$\omega_f$ = free frequency

$\omega_1$ = forced frequency

$\omega_{fo}$ = unperturbed free frequency

$\doteq (1 - \frac{\alpha^2}{16})$

Hence the frequency deviation at critical locking is given by:

$$\omega_f - \omega_{fo} = \frac{\alpha^2}{16} \frac{(\omega_1^2 - \frac{1}{2})}{\omega_1(\omega_1 - 1)} \qquad (22)$$

where the frequencies are normalized with respect to $\omega_o = 1$.

This may be compared with the deviation calculated by van der Pol[1] where

$$\omega_f - 1 = \frac{\alpha^2}{32(\omega_1 - 1)} \qquad (23)$$

is the frequency deviation from $\omega_o$ (normalized to 1).

If the free running frequency is taken as $(1 - \frac{\alpha^2}{16})$, then equation (23)) becomes:

$$\omega_f - \omega_{fo} = \frac{\alpha^2}{16} \frac{(\omega_1^2 - \frac{\omega_1}{2})}{\omega_1(\omega_1 - 1)} \tag{24}$$

although it is questionable to do this since to the order of accuracy of van der Pol's solution the free running frequency is $\omega_o$. (This is because only the fundamental component of the nonlinear element output was considered).

The analysis can be extended to include the third harmonic of the forced oscillation. In this case,

$$e_o = E_1 \cos \omega_1 t + E_3 \cos (3\omega_1 t + \phi)$$

and the variational equation (17) becomes

$$\frac{d^2\xi}{dt^2} - \alpha \{1 - \beta\frac{E_1^2}{2} - \beta \frac{E_1^2}{2} \cos 2\omega_1 t - \beta E_1 E_3(\cos(4\omega_1 t + \phi) + \cos(2\omega_1 t + \phi))\} \omega_o \frac{d\xi}{dt} + \{\omega_o^2 - \alpha\beta\omega_o [\omega_1 E_1^2 \sin 2\omega_1 t + E_1 E_3 (4 \sin (4\omega_1 t + \phi) + 2 \sin (2\omega_1 t + \phi))]\} \xi = 0 \tag{25}$$

and the variation $\xi$ is taken as

$$\xi = A_1 \sin (\omega_f t + \psi) + B_1 \sin ((2\omega_1 - \omega_f)t + \theta) + A_3 \sin (3\omega_f t + \varepsilon) + B_3 \sin ((4\omega_1 - \omega_f)t + \Theta)$$

The method is similar to the previous solution, although the algebra is rather lengthy, the solution is:

$$\omega_f - \omega_{fo} = \frac{\alpha^2}{16} \frac{\omega_1^2}{(\omega_1^2 - 1)} \qquad (26)$$

These three formulae were compared numerically, and the results are given in the table below, with $\omega_o$ normalized to 1.

| $\omega_1$ | Equation (22) | Equation (26) | Equation (24) (van der Pol) | Experimental |
|---|---|---|---|---|
| 0.694 | $0.036 \times 10^{-3}$ | $-0.388 \times 10^{-3}$ | $-0.265 \times 10^{-3}$ | $-2.78 \times 10^{-3}$ |
| 0.926 | -2.130 " | -2.510 " | -2.38 " | -6.02 " |
| 1.158 | 1.921 " | 1.644 " | 1.741 " | 3.14 " |
| 1.390 | 1.104 " | 0.866 " | 0.954 " | 1.20 " |
| 1.621 | 0.883 " | 0.675 " | 0.755 " | 0.787 " |
| 1.851 | 0.777 " | 0.590 " | 0.664 " | 0.671 " |
| 2.084 | 0.711 " | /0.543 " | 0.611 " | 1.16 " |

The values taken for $\omega_1$ correspond to the frequencies used in the experimental curves of Figure 4.6, and $\alpha$ was taken as $\alpha = 0.0819$, the value used experimentally.

### 3.2-3 Frequency of the Free Oscillation for Small Disturbances

For small disturbances, $e_o$ in the variational equation, equation (17), is set equal to the free running undisturbed output, which is (Chapter 2 and Appendix A) given by

$$e_o = \frac{2}{\sqrt{\beta}} \cos \varphi t$$

The variational equation then becomes, with β normalized to 1

$$\ddot{\xi} + \alpha[1 + 2\cos 2\omega_f t]\omega_o\dot{\xi} + [\omega_o^2 - 2\alpha\omega_o\omega_f \sin 2\omega t]\,\xi = -\left(\frac{I\omega_1}{C}\right)\sin\omega_1 t \tag{27}$$

Since the free running solution was used for $e_o$, the right hand forcing term is not cancelled.

In this case it is expedient to choose (paragraph 3.4)

$$\xi = A\sin(\omega_1 t + \psi) + B\sin((2\omega_f - \omega_1)t + \theta) \tag{28}$$

which are the two main sidebands.

Substituting this into the variational equation, and equating the coefficients of $\sin\omega_1 t$, $\cos\omega_1 t$, $\sin(2\omega - \omega_1)t$ and $\cos(2\omega - \omega_1)t$ separately to zero yields the four equations, written in matrix form as:

$$\begin{bmatrix} 1-\omega_1^2/\omega_o^2 & -\alpha\omega_1/\omega_o & 0 & -\alpha\omega_1/\omega_o \\ \alpha\omega_1/\omega_o & 1-\omega_1^2/\omega_o^2 & -\alpha\omega_1/\omega_o & 0 \\ 0 & -\alpha(2\omega_f-\omega_1)/\omega_o & 1-(2\omega_f-\omega_1)^2/\omega_o^2 & -\alpha(2\omega_f-\omega_1)/\omega_o \\ -\alpha(2\omega_f-\omega_1)/\omega_o & 0 & (2\omega_f-\omega_1)/\omega_o & 1-(2\omega_f-\omega_1)^2/\omega_o^2 \end{bmatrix} \tag{29}$$

$$\times \begin{bmatrix} A\cos\psi \\ A\sin\psi \\ B\cos\theta \\ B\sin\theta \end{bmatrix} = \begin{bmatrix} -\frac{I\omega_1}{C\omega_o^2} \\ 0 \\ 0 \\ 0 \end{bmatrix}$$

which is similar to equation (20), but has fewer zero elements. For convenience the time scale has been normalized as in Chapter 2 i.e. $t \to \frac{t}{\omega_o}$. To simplify the algebra, we make the substitutions:

$$a = \omega_1/\omega_o$$

$$b = (2\omega - \omega_1)/\omega_o$$

and normalize $\beta = 1$.

The equation becomes:

$$\begin{bmatrix} 1-a^2 & -\alpha a & 0 & -\alpha a \\ \alpha a & 1-a^2 & -\alpha a & 0 \\ 0 & -\alpha b & 1-b^2 & -\alpha b \\ -\alpha b & 0 & \alpha b & 1-b^2 \end{bmatrix} \begin{bmatrix} A\cos\psi \\ A\sin\psi \\ B\cos\theta \\ B\sin\theta \end{bmatrix} = \begin{bmatrix} -\frac{Ia}{C\omega_o} \\ 0 \\ 0 \\ 0 \end{bmatrix}$$

The magnitudes and phases of the sidebands can now be found.

Hence,

$$\begin{aligned} A\cos\psi &= -\frac{I}{C\omega_o}\, a\left[(1-a^2)((1-b^2)^2 - \alpha^2 b^2) - \alpha^2 ab(1-b^2)\right]/\Delta \\ A\sin\psi &= \alpha\frac{I}{C\omega_o}\, a^2(1-b^2)^2/\Delta \\ B\cos\theta &= \alpha^2\frac{I}{C\omega_o}\, b\left[a(1-b^2) - b(1-a^2)\right]/\Delta \\ B\sin\theta &= -\alpha\frac{I}{C\omega_o}\, ab(1-a^2)(1-b^2)/\Delta \end{aligned} \qquad (30)$$

where $\Delta$ is the determinant of the coefficients

$$\Delta = \left[(1-a^2)^2 + \alpha^2 a^2\right]\left[(1-b^2)^2 + \alpha^2 b^2\right] - 2\alpha^2 ab(1-a^2)(1-b^2) - \alpha^4 a^2 b^2$$

The solution may be written (with $\beta$ normalized to 1) as:

$$\begin{aligned} e &= e_o + \xi \\ &= 2\cos\omega t + A\sin(\omega_1 t + \psi) + B\sin((2\omega-\omega_1)t + \theta) \end{aligned} \qquad (31)$$

with A and B given by equations (30).

We now return to the van der Pol equation, equation (2) to obtain the final relation needed to find the frequency.

If equations (30) are substituted into equations (2), and the coefficient of cos ωt equated to zero, the following equation is obtained:

$$\frac{\omega}{\omega_o}f^2 - 1 - \frac{\alpha}{2}(A\sin\psi\ B\cos\theta + A\cos\psi\ B\sin\theta)\frac{\omega}{\omega_o}f = 0 \qquad (32)$$

Since $A\sin\psi\ B\cos\theta << A\cos\psi\ B\sin\theta$, this is approximately

$$\frac{\omega}{\omega_o}f^2 - 1 - \frac{\alpha}{2}\ A\cos\psi\ B\sin\theta\ \frac{\omega}{\omega_o}f = 0 \qquad (33)$$

Ignoring powers of α greater than $\alpha^2$

$$A\cos\psi\ B\sin\theta = \alpha\left(\frac{I^2}{C^2\omega_o^2}\right)\ \frac{a^2b}{(1-a^2)^2(1-b^2)}$$

The frequency deviation is small, so we look for a root of $\frac{\omega}{\omega_o}$ near 1.

Let $\frac{\omega}{\omega_o}f = 1 + \delta$ where $\delta = \frac{\omega_f - \omega_{fo}}{\omega_o}$

$$b = (2 - a) + 2\delta$$

$$b^2 = (2 - a)^2 + 4\delta(2 - a)$$

Equation (33) then becomes:

$$2\delta - \frac{\alpha^2}{2}\left(\frac{I}{\omega_o C}\right)^2 \frac{a^2(2-a + 2\delta)(1 +\delta)}{(1-a^2)^2(1-(2-a)^2 - 4\delta(2-a))} = 0$$

Ignoring terms in $\delta^2$, the solution is found to be:

$$\omega_f - \omega_{fo} = \omega_o\ \frac{\alpha^2}{4}\ \beta\left(\frac{I}{\omega_o C}\right)^2\ \frac{a^2(2-a)\ (1 + (2-a)^2)}{(a-1)^3(1+a)^2(3-a)^2} \qquad (34)$$

with the amplitude normalizing parameter β reinserted. Values obtained from equation (34) are tabled below, and correspond with the frequencies experimentally used, in Figure 4.7.

| INPUT FREQUENCY | a | EQUATION (34) | EXPERIMENTAL |
|---|---|---|---|
| 150 KHz | .694 | -3.74 Hz | -1.7Hz |
| 200 | .926 | -314. | -74. |
| 250 | 1.158 | 29.6 | 14. |
| 300 | 1.390 | 1.8 | 1.7 |
| 350 | 1.621 | .34 | .29 |
| 400 | 1.851 | .08 | .02 |

$\frac{\omega_o}{2\pi}$ = 216 kHz  I = $10^{-1}$ mA(peak)  C = 780 pF  α = .0819

## 3.3 Elementary Approach for a Large Narrow Band Noise Input:

When white noise is passed through a narrow band filter, it can be shown that the output is of the form[22]

$$v(t) = V(t) \cos (\omega_n t + \phi(t))$$

where $\omega_n$ is the filter centre frequency, and $V(t)$ and $\phi(t)$ are slowly varying random time functions, varying with a maximum frequency of $\Delta f$, the filter bandwidth. The double sided spectrum $S(f)$ is of the type:-

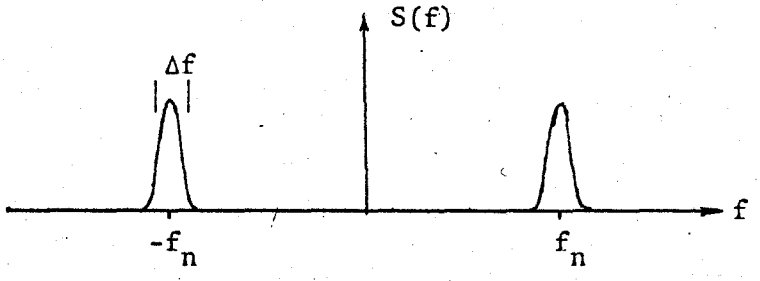


The probability density functions for $V(t)$ and $\phi(t)$ are found to be[22]

$$p(V_t) = \frac{V_t}{\sigma^2} e^{-\frac{V_t^2}{2\sigma^2}} \qquad V_t \geq 0$$

$$= 0 \qquad \text{otherwise}$$

$$p(\phi_t) = \frac{1}{2\pi} \qquad 0 \leq \phi \leq 2\pi$$

$$p(V_t, \phi_t) = \frac{V_t}{2\pi\sigma^2} e^{-\frac{V_t}{2\sigma^2}}$$

where

$V_t$ = sample function of $V(t)$

$\phi_t$ = sample function of $\phi(t)$

$\sigma$ = root mean square value of $V_t$

It should be noted that while $V_t$ and $\phi_t$ are independent random variables, the processes yielding them are not independent. See Reference 22.

The cumulative distribution for $V_t$ is:

$$P(V_t \leq V_e) = \int_0^{V_e} \frac{V_t}{\sigma^2} e^{-\frac{V_t^2}{2\sigma^2}} dV_t = 1 - e^{-\frac{V_e^2}{2\sigma^2}}$$

Now if $\sigma$ is large, the noise input to the oscillator will rise above the value required for synchronization, and the oscillator will lock onto it. When it drops back below this value, the free oscillations will recommence. Thus from the above, the proportion of the time the oscillator is locked can be found, and the net frequency is then;

$$f = P(V_t \geq V_e)\ f_n + (1 - P(V_t > V_e))\ f_o \qquad (35)$$

where $f_o$ = oscillator unperturbed frequency.

The assumptions are that the oscillator locks and unlocks instantaneously onto $V_t$, and returns to its free running frequency when unlocked.

Neither of these assumptions are true. The oscillator required of the order of 200 cycles to lock or unlock (the unlocking transient is slightly faster than the locking transient, but both are of this order). Also the oscillator does not drop back to $f_o$ in the unlocked condition, but to some frequency near $f_o$, depending on the magnitude of the noise. The error, however, becomes insignificant when an appreciable proportion of the time is spent in the locked condition.

The approach does not hold if $f_n \approx nf_o$ ($n = \text{----} \frac{1}{3}, \frac{1}{2}, 0, 1, 2, \text{--}$) since resonances will occur.

If the rms magnitude of the noise is low, the time spent above the locking value becomes very small, and the oscillator rarely becomes synchronized. In this case the frequency shift of the oscillator is due almost entirely to the pulling effect seen in the sine wave disturbance case, paragraph (4.6). Calculation shows that the knees in the curves of Figures 4.5 and 4.6 occur when the magnitude of the narrow band noise is large enough so that it remains above the critical locking value for several hundred cycles, allowing synchronization to occur.

Figures 4.5 and 4.6 are graphs of the frequency deviation from the free frequency against the rms magnitude of the input noise current. Also plotted (dashed curves) are the curves obtained from Equation (35).

It can be seen that agreement is at best only fair; curves for noise of centre frequency below 125 kHz were not plotted as the agreement was very poor.

However, considering the difficulties in obtaining the curves, and also in obtaining the data for the calculation, the agreement is remarkable, and shows that a random locking phenomena in fact occurs.

## 3.4 Discussion of the Methods

The method of A. W. Gillies[12a] is of some interest since theoretically it is possible to consider the effect of as many harmonics as desired. However, as has been found in practice, the algebra becomes rapidly intractable. The solution is in the form of a series, equation (11), and it is difficult to ascertain its convergence. The frequency deviation is, however, proportional to $i^2$ over the rising part of the curve (Figure 3.1 curve 2), although the empirical relation

$$\text{Frequency Shift} \propto \frac{1}{\left(\frac{\omega_1}{\omega_o} - 1\right)^3}$$

obtained in paragraph 4.7 does not hold when $\omega_1$ is varied in Gillies'[12a] formulae. The method does, however, show the importance of the higher order modulation terms, and indicates that the seventh order terms may be significant.

The variational technique of using a known solution to find a better higher order solution is also useful; Hafner's[11] method being of this type.

The variational equation used in paragraph 3.2-2 is different from that used in paragraph 3.2-3 in that the right hand forcing term F(t) has been cancelled by the first order solution, and that in paragraph 3.2-3 has not. This means that in 3.2-2 we are not obtaining a "better" solution when the oscillator is just locked, rather we are introducing a perturbation $\xi$ at the output and examining the nature of this perturbation to find its frequency; while in 3.2-3 we are examining the variation in the output due to a small perturbing input.

The choice of $\xi$ is of significance. Consider the variational equation (18). If we assume $\xi = A \sin \omega t$ in paragraph 3.2-1, modulation frequencies of $\omega$ and $2\omega_1 - \omega$ are produced after the substitution of $\xi$, and the frequency $2\omega_1 - \omega$ cannot intermodulate to produce $\omega$. It can be seen that in this case, the solution is $\omega = \omega_o$ and there would be no frequency shift (from inspecting equation (20)). Therefore, if frequencies $\omega$ and $\omega_1$ are present, so also must the frequency $2\omega_1 - \omega$, and this has to be recognized in the choice of $\xi$. Thus, if $\xi$ is chosen as

in equation (19), the required third order modulation product of frequency $\omega$ will result.

A similar argument for the free running oscillator will show that the third harmonic, $3\omega$, in the output (Chapter 2) intermodulates in the nonlinear element to produce a current of frequency $\omega$, but having a different phase than the first order component. The resonant circuit must then be slightly reactive to restore the phase shift round the circuit to zero, which causes the slight lowering of the frequency from $\omega_o$ to $\omega_o - \frac{\alpha^2}{16}\,\omega_o$.

The same reasoning applies to paragraph 3.2-2, the term of frequency $2\omega - \omega_1$ is necessary to obtain the third order modulation product of frequency $\omega$, whose phase determines the frequency of the fundamental. The phase angle included with the frequency $2\omega - \omega_1$ is necessary because this frequency originates from the third order modulation products of $\omega$ and $\omega_1$, and its phase is thus related to the phases of these frequencies. The phase angle $\psi$ associated with $\omega_1$ is the phase angle between the driving current and resulting voltage of this frequency. Equation (29) can also be obtained directly from the van der Pol equation (2); the procedure is the same, but substituting equation (28) into equation (2) instead of the variational equation (27), and neglecting $B^2$ compared to the squared amplitude of the fundamental. If the third harmonic is included, that is

$$e' = e + D\sin(3\omega t + \lambda)$$

then the expression in parenthesis of equation (32) contains the additional terms:

$$\frac{\omega}{\omega_o} \; D \cos \lambda + \frac{ABD}{2} \; \frac{\omega_1}{\omega_o} \; \cos (\lambda - \theta - \psi)$$

The first term, with $D \cos \lambda = - \alpha \frac{E}{8}$, E = normalized free running amplitude (Chapter 2), gives the constant deviation of $- \frac{\alpha^2}{16} \omega_o$ from $\omega_o$.

This is evident also in Gillies'[12a] solution, curve(2) (Figure 3.1) including the third harmonic (represented by the presence of $\zeta_{3a}$ in equation (11)) shows zero deviation from the free running frequency while curve 1 (which does not include $\zeta_{3a}$) gives the free running frequency as $\omega_o$, that is, a deviation of $\frac{\alpha^2}{16} \omega_o$ from the actual. The second term is of order $\alpha^2$ and so can be neglected to the order of approximations used in 3.3-2. Additional terms to the above are introduced by considering the two sidebands about $3\omega_3$, of frequency $2\omega + \omega_1$ and $4\omega - \omega_1$, but these are of order $\alpha^2$, also.

The agreement with experiment is only fair, as can be seen from the table of equation (34). Qualitatively, the triple pole at (a - 1) is in experimental agreement, as is the fact that the frequency deviation is proportional to the square of the input perturbation.

Stover's [21] observation of the assymmetric sideband distribution can be explained in terms of the above theory, by noting that A (paragraph 3.2-2 or 3.2-1) is an order of $\alpha$ higher than B. Carrying this further, consider an output with frequencies $\omega$, $\omega_1$. These will intermodulate in the nonlinear element and produce the sideband $(2\omega - \omega_1)^{(\alpha)}$ where $^{(\alpha)}$ indicates that this sideband has a magnitude of order $\alpha$. Now consider an output of frequencies $\omega$, $\omega_1$, $(2\omega - \omega_1)^{(\alpha)}$. These will

similarly intermodulate and produce $3\omega^{(\alpha^2)}$, $(3\omega - 2\omega_1)^{(\alpha^2)}$ as additional frequencies. Thus it can be seen that the sidebands on the side of the fundamental opposite the driver are of the same order as those on the same side as the driver. Furthermore, each sideband is $\alpha$ times its neighbour nearer the fundamental, also observed by Stover[21].

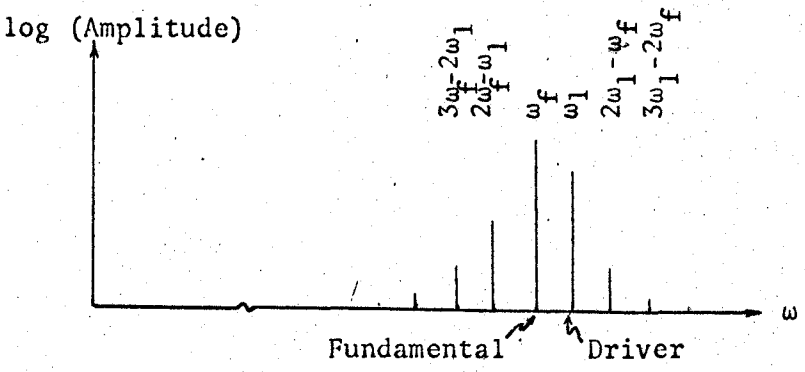

# CHAPTER IV

# EXPERIMENTAL INVESTIGATION

The nonlinear oscillator circuit of Figure (4.1) was set up to experimentally examine the van der Pol oscillator.

## 4.1 Oscillator Circuit:

The non-linear element was simulated by using the cathode coupled double-triode circuit of V3 in Figure (4.1). The first stage, a cathode follower, feeds the second, a common grid amplifier, which provides the inversion necessary for negative resistance operation.

To obtain the cubic form required, the tubes were biased near cut-off, so that one, V2b, cut-off on the positive half cycle and V2a on the negative half cycle. By adjusting the cathode resistor, the amount of cut-off could be varied, which corresponds to varying the cubic coefficient b in the nonlinear resistance characteristic,

$$i = -ae + be^3$$

The resistor shunting the circuit can be altered to change the resultant value of a.

The voltage / current characteristic of the circuit could be displayed on an oscilloscope using the 100Ω resistor for the current measurement.

Also in the circuit is a potentiometer chain which changes the relative biassing of the two tubes. This is necessary to ensure that the

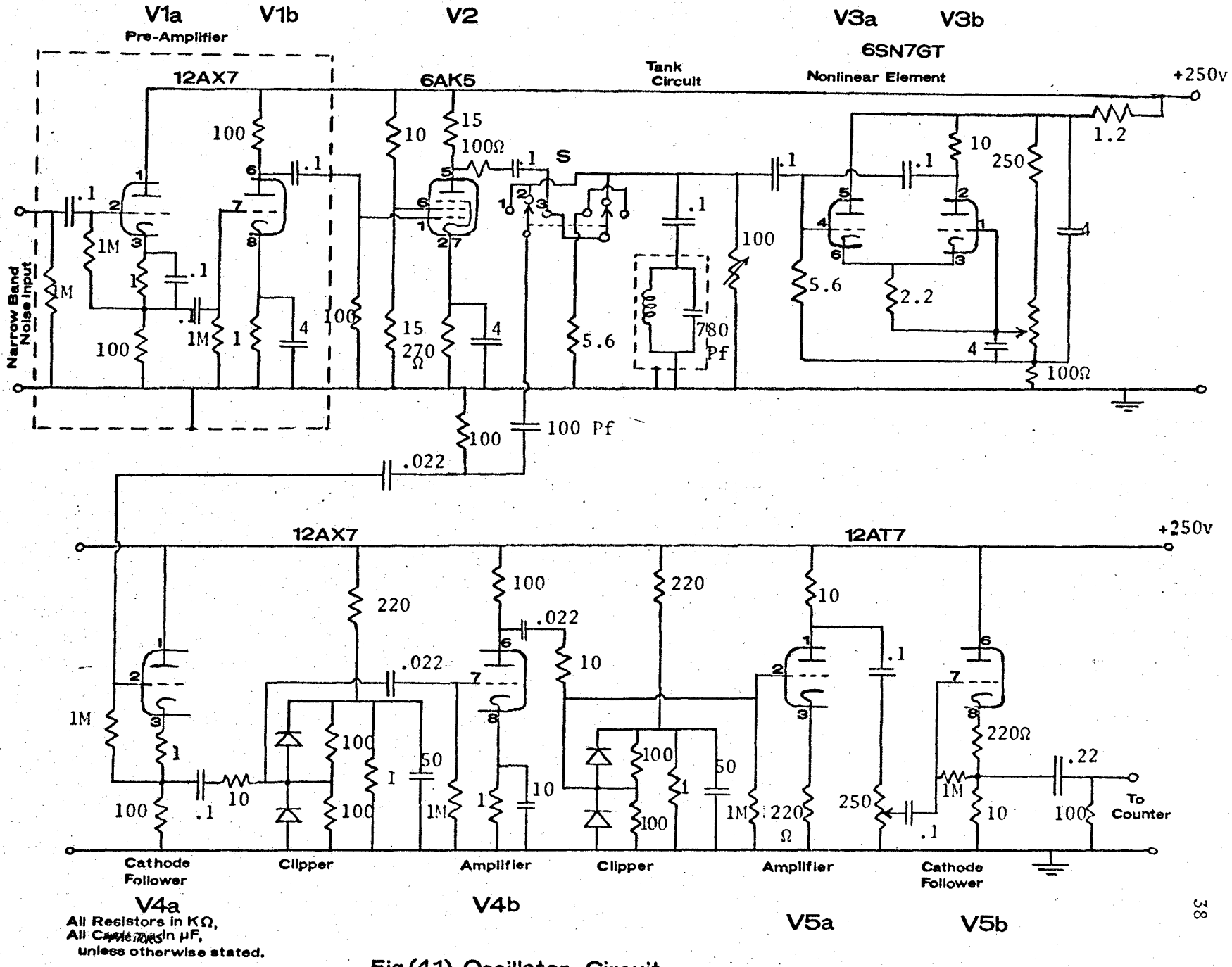


Fig.(4.1) Oscillator Circuit.

characteristic is symmetrical, that is, there is no $e^2$ term in the non-linear characteristic. This can be adjusted by examination of the oscilloscope characteristic, but it was found that a more accurate setting could be obtained by examining the free running oscillator for any second harmonic. By very careful adjustment, the second harmonic content of the oscillator was reduced to less than 0.1%. When doing this, the filter must be connected directly to the oscillator, since a buffer amplifier will introduce enough second harmonic to mask that of the oscillator.

The oscillator circuit was completed by adding the LC tank circuit as shown.

Tubes were used rather than transistors because of the better aging characteristics, and the better input/output isolation. When transistors were tried it was found that the junction capacitance varied with time and temperature to give a random frequency drift in the oscillator output. This was largely avoided by using tubes, and allowing the oscillator to warm up for several days while enclosed in a box to exclude draughts. The oscillator was also mounted on shock absorbant material to avoid microphonics.

## 4.2 Noise Source:

The narrow band noise source was obtained by passing white noise from a noise generator through a narrow band filter. The filter consisted of a simple L.C. circuit, as shown below in Figure (4.2).

A coil of 1.71 mH (using Ferroxocube) gave a Q factor > 100 up to 150 KHz and a coil of 356 μH (Mullard) gave Q > 100 from 150-400 KHz,

thus covering the entire range of interest.

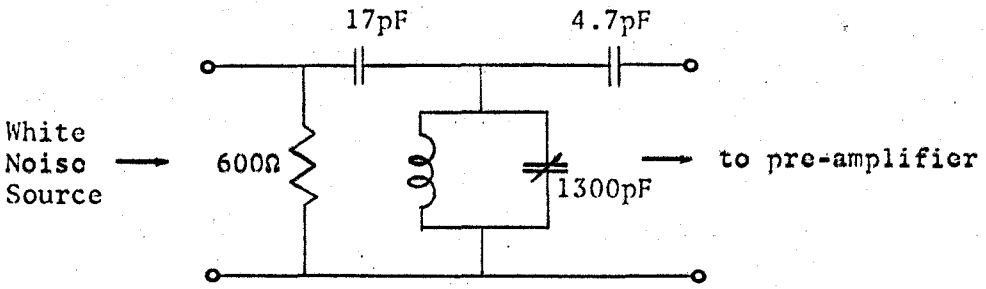


FIGURE 4.2

4.3 Input/Output Circuits:

(i) Input-

The noise filter output was fed into a preamplifier V1, Figure 4.1. The 12AX7 is a high-μ double triode tube, whose output was fed to the pentode current-source driver stage V2. V2 was biassed at 11 mA and it was found that it delivered up to 2 mA rms of signal current before saturation effects occurred, and that 2.5 mA would be delivered before this became serious.

(ii) Output-

It was found that the direct connection of measuring instruments (voltmeter, counter, etc.) to the oscillator affected the oscillator frequency and amplitude. An output buffer amplifier was therefore provided.

This consisted of a high pass (8 KHz) RC filter feeding a cathode follower as in Figure 4.1. Thus a constant output load was presented to the oscillator, independent of the various meter settings. For the larger values of input noise, the oscillator output was found to be highly amplitude modulated, and as the counter used did not count

small inputs, the wave was clipped and amplified by the clipper circuits shown, to produce an approximately square wave output, of the frequency of the zero crossings of the input.

Alternatively, the frequency of the fundamental could be measured by inserting a band pass filter after the cathode follower V4a, although in this case, care had to be taken that the resulting phase shift in the clipper circuits did not feed itself back to the oscillator, by capacitive or inductive coupling in the wiring for example, and thus affect the free running frequency.

4.4 Measurement of Circuit Parameters:

The parameters to be determined are L, C, and a, b—the negative resistance parameters. These parameters must be determined under working conditions, that is, with the input and output buffer amplifiers connected.

$i = -ae + be^3$

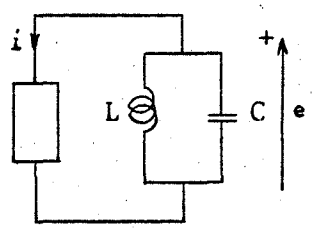


The values of L, C and the Q factor of the coil were found using a Q-meter.

The values of a and b can be found from the geometry of the nonlinear resistance characteristic which can be displayed on an oscilloscope (Figures 4.3 and 4.4).

$i = -ae + be^3$

$\frac{di}{de} = -a + 3be^2$

$= 0$ at turning points, A and B.

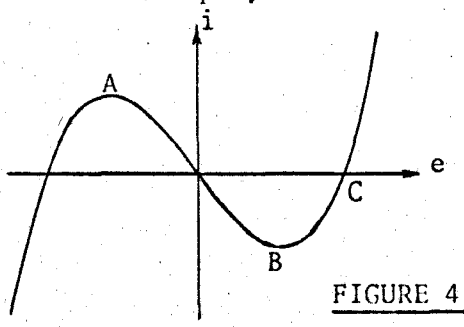


FIGURE 4.3

$i = -ae + be^3$

Hence $a = 3be^2$ and we find:

$$\left.\begin{aligned} b &= \frac{-i}{2e^3} \\ a &= 3be^2 \end{aligned}\right\} \text{ at the turning points A and B.}$$

Also at Point C $i = 0$, $e = \sqrt{\frac{a}{b}}$.

Values found in this way were:

$$a = 0.25 \times 10^{-3} \ \mho$$

$$b = 8.70 \times 10^{-6} \ \mho V^2$$

The value of "a" obtained in this way must be modified to

$$a \rightarrow a - \frac{1}{R_i}$$

in order to be of use in calculations. $R_i$ is a distributed resistance made up of the input and output buffer amplifier resistances and the (neglected) tank shunt resistance.

It is known that in the free running state, the oscillation amplitude is:

$$E = \sqrt{\frac{4(a - \frac{1}{R})}{3b}}$$

where R is an external shunt, and a is the modified value.

$$E^2 = \frac{4a}{3b} - \frac{4}{3b}\ \frac{1}{R}$$

If $E^2$ is plotted against 1/R a straight line, slope $-\frac{4}{3b}$, intercept "a" on the 1/R axis, should result. This was done; the oscillator was shunted with various known resistors and the amplitude noted. The resultant graph was linear, and gave the values below which are the values used in the calculations. The error in the value of "a" was estimated

to be 2%, and that of b to be 15%.

$$a = .088 \times 10^{-3}\ \mho$$
$$b = 8.72 \times 10^{-6}\ \mho/V^2$$

The value of b was adjusted within its range of error so that the free running amplitude was:

$$3.67 = \sqrt{\frac{4a}{3b}}$$

which is the measured value.

An attempt was made to measure the parameters by measuring the harmonics in the oscillator output and calculating a and b from the second order harmonic balance solution (paragraph 2.2),

$$e = E \cos \omega_o t + \frac{\alpha E}{8} (3 \sin \omega_o t - \sin 3\omega_o t)$$

where

$$\alpha = \frac{a}{C\omega_o} \quad \text{and} \quad E = \sqrt{\frac{4a}{3b}}$$

The harmonics could not however be determined with sufficient accuracy. This was because the measuring instruments had to be connected directly to the oscillator, which altered the operating parameters. A buffer amplifier introduced a spurious second harmonic, and as the third harmonic content is only about 1%, and the attempt was abandoned.

In summary, the parameters were found to be;

$$[a = .25 \times 10^{-3}\ \mho \text{(N.L.R. only)}]$$
$$a = 0.088 \times 10^{-3}\ \mho \text{ (overall circuit)}$$
$$b = 8.72 \times 10^{-6}\ \mho/V^2$$

$$\sqrt{\frac{4a}{3b}} = 3.67 \text{ volts}$$

and C = 780 pF. $\omega_o$ = 216 KHz.

Hence, the constants of the van der Pol equation for the oscillator are:

$$\alpha = 0.0819$$

$$\beta = 0.297$$

4.5 Experimental Technique:

The frequency shift of the forced oscillator from its free running frequency was investigated experimentally. Since random frequency drifts due to thermal or other effects could never be completely eliminated, these had to be allowed for by taking the mean of the free running frequency before and after a measurement.

The procedure was as follows:

(i) The switch S (Figure 4.1) was turned to position 1. This places the output of the pentode across a known resistor, so that by measuring the voltage at this point, the effective current source strength can be found. The level was set to a small value by adjusting the noise generator gain control.

(ii) The noise generator was disconnected from the narrow band filter and switch S turned to position 2. The frequency of the free running oscillator was measured by the counter, using a ten second gate time, several readings being made.

(iii) The noise generator was reconnected to the narrow band filter, and several readings of the perturbed frequency taken.

(iv) The noise generator was again disconnected and the free running frequency again recorded.

The mean frequency deviation is then the average of (ii) and (iv) less the average of (iii).

This procedure was repeated for other input values and also at other noise centre frequencies. The filter was tuned using a (sine wave) oscillator.

When a sine wave was used as a forcing function instead of narrow band noise, the narrow band filter was still kept in the circuit as it acted as an attenuator pad, isolating the external oscillator, and filtering switching transients which sometimes caused a jump in the oscillator free running frequency. The (fluorescent) room lighting was turned off as trouble was experienced with mains hum.

## 4.6 Experimental Results:

The results of the experimental work are given in graphical form in Figures 4.5, 4.6, and 4.7. These are graphs of the deviation of the oscillator frequency from the free running frequency against the magnitude of the input disturbance. The frequency was measured by counting the number of zero crossings (obtained from the clipping circuits of Figure 4.1 ) over ten seconds and dividing by two.

Figures 4.5 and 4.6 are with a narrow band noise input and Figure 4.7 with a sine wave input. The curves of Figure 4.7 terminate at the point of synchronization when the amplitude of the free oscillation becomes zero. Figure 4.4 shows some experimental waveforms.

## 4.7 An Empirical Result:

The curves of Figure 4.7 are replotted in Figure 4.8 on log-log scales, and it can be seen that these are approximately straight lines, for small inputs. The curves deviate from a straight line for

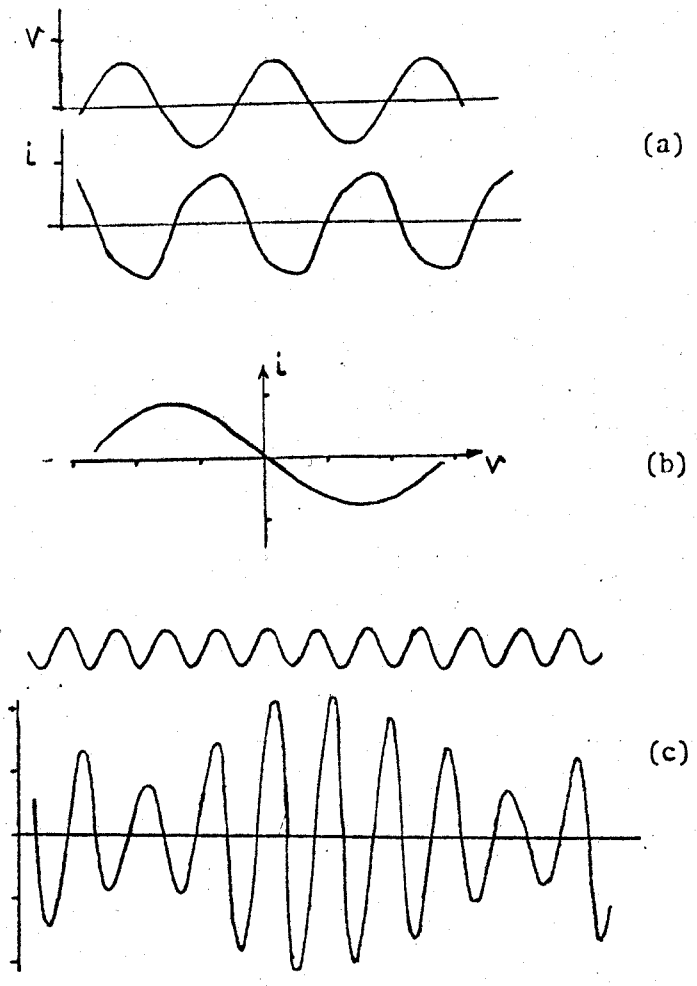


FIGURE 4.4 Experimental Waveforms

(a) Voltage and current waveforms for the nonlinear element in the free running oscillator. Scales are:

v - 5v/div
i - 0.5 ma/div

(b) Voltage/current characteristic of the nonlinear element. Scales are:

v - 2.16 v/div
i - 0.5 ma/div

(c) Output waveform of the forced oscillator. The upper wave is the input current of 0.5 mA (peak) at 250 KHz. and the lower is the oscillator output voltage waveform, scale 2v/div. This can be compared with the computed waveform, Figure C2.

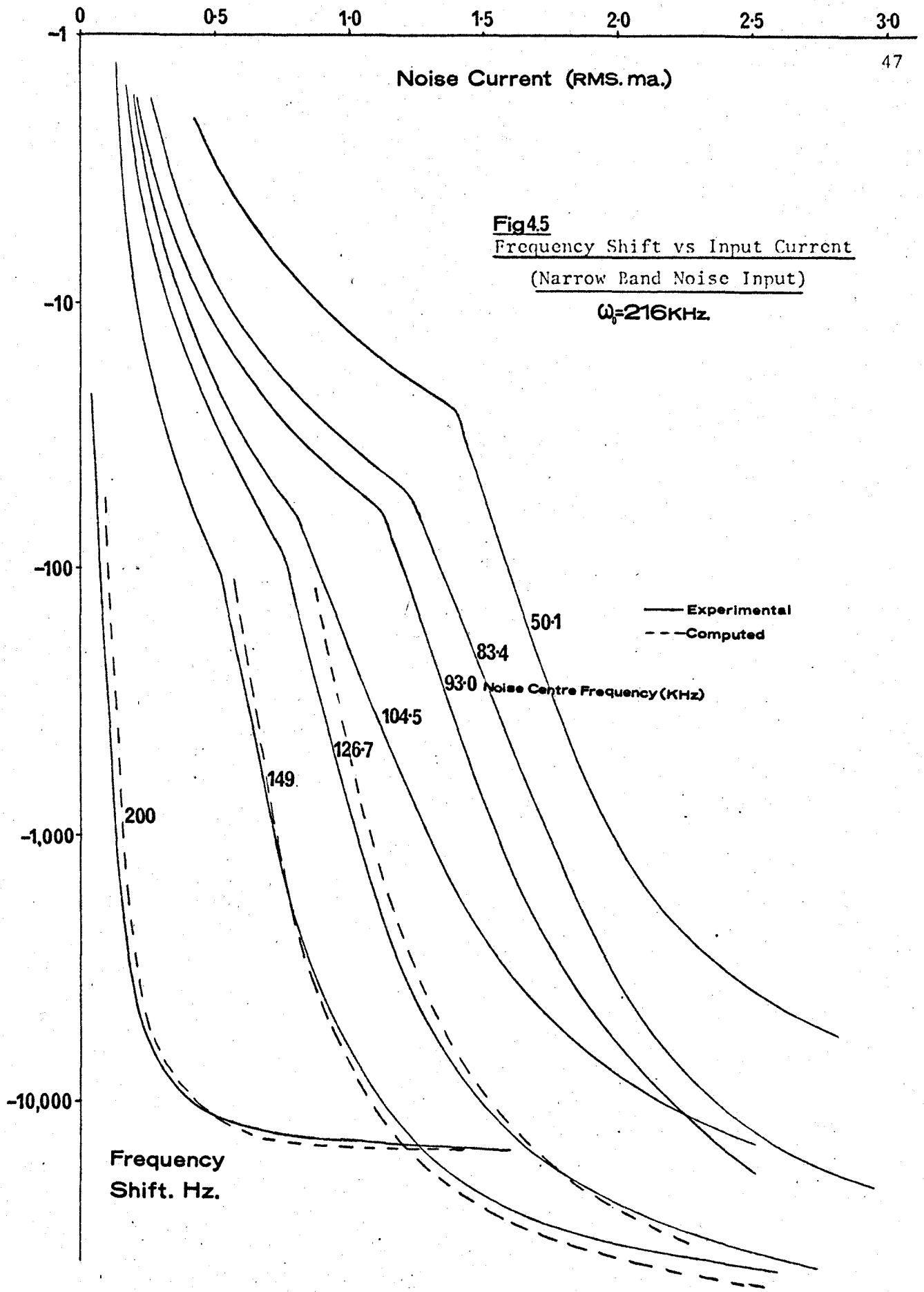


Fig 4.5
Frequency Shift vs Input Current
(Narrow Band Noise Input)
$\omega_0$=216KHz.

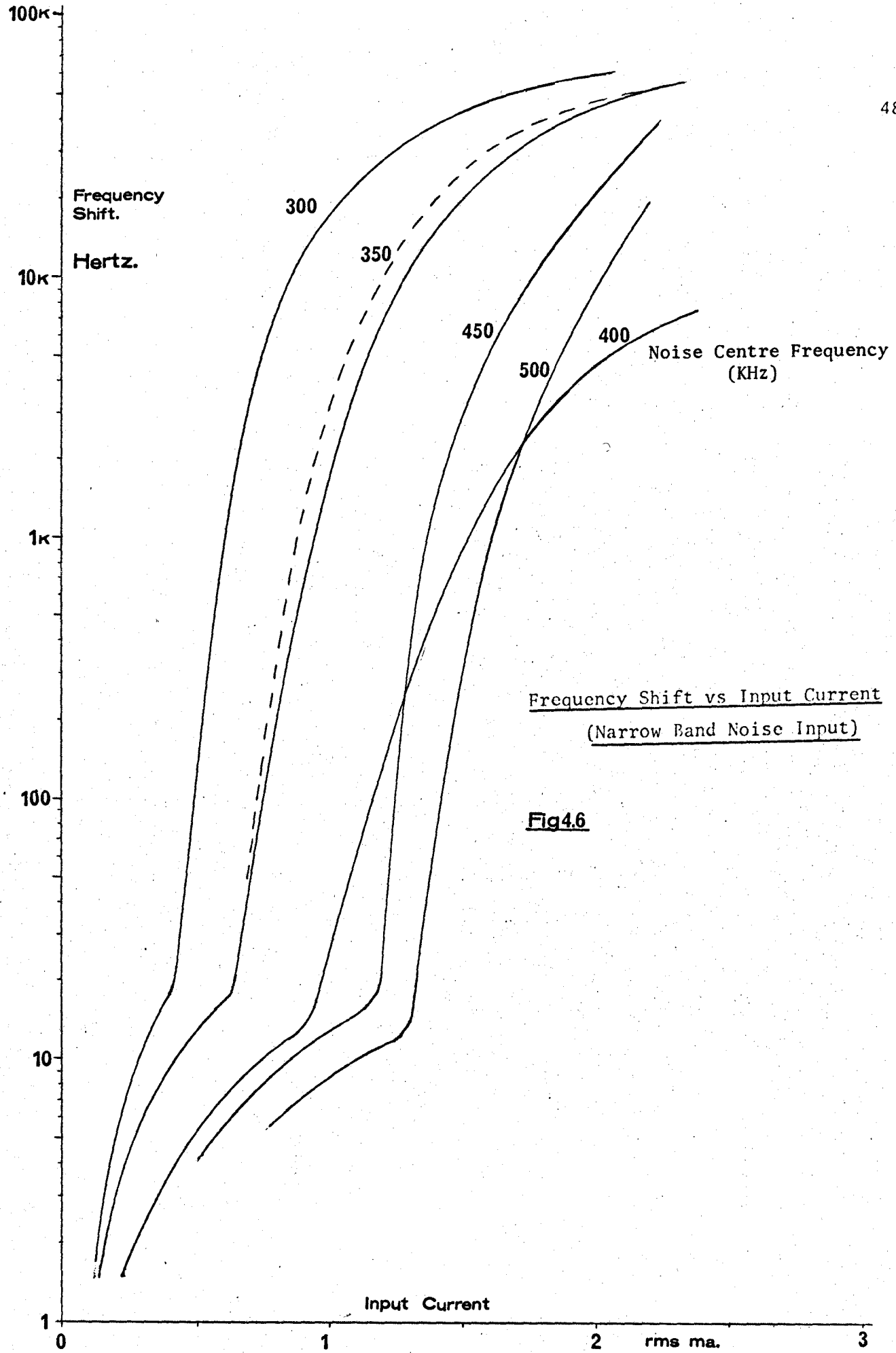


Frequency Shift vs Input Current

(Narrow Band Noise Input)

Fig4.6

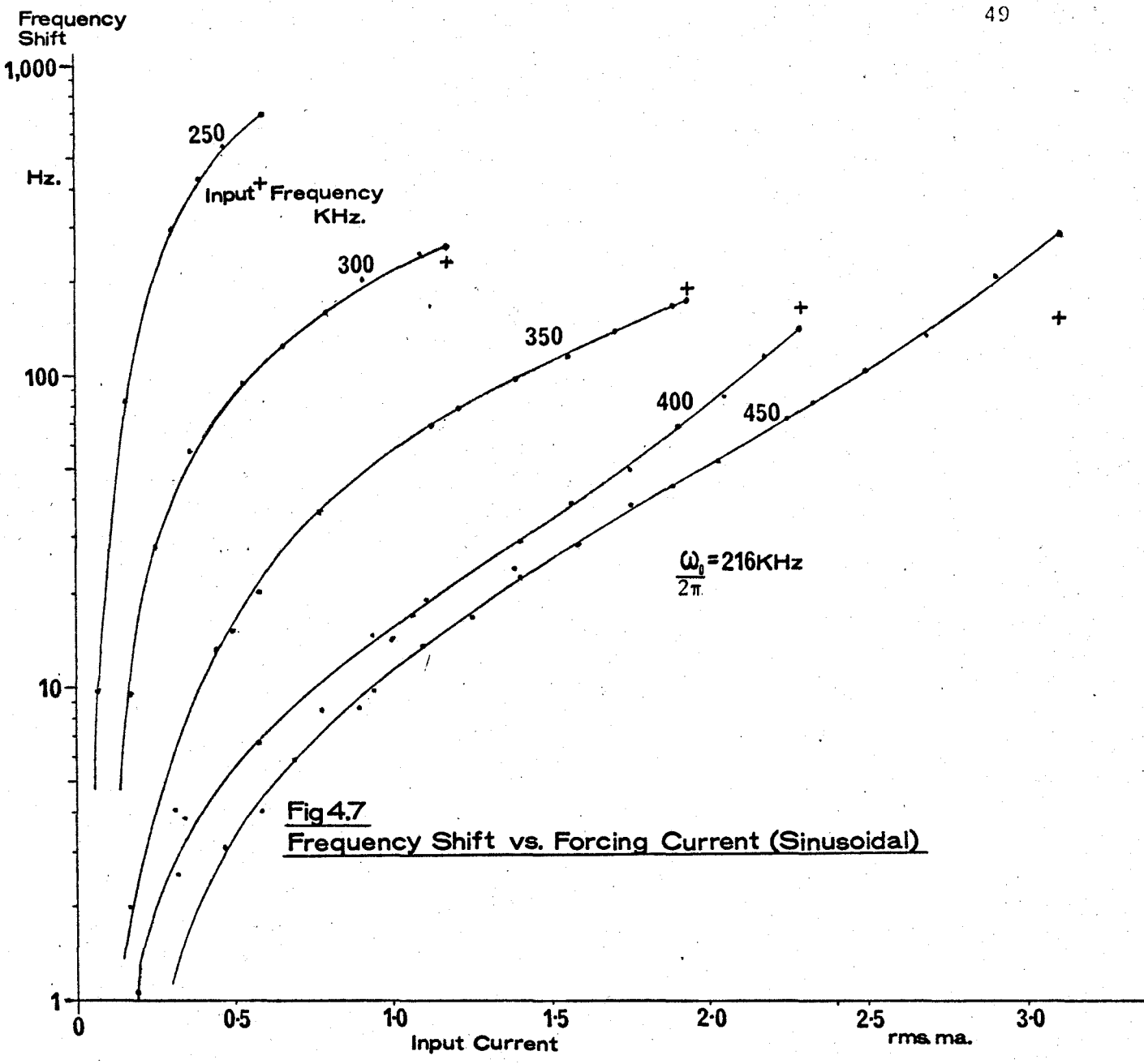


Fig 4.7
Frequency Shift vs. Forcing Current (Sinusoidal)

large inputs. This is particularly marked in the curve for $\omega_1$ = 400 KHz. The cause of this is not known, but it may be noted that this frequency is near the second harmonic of the fundamental, and so may thus introduce effects unimportant at other frequencies. For example, there will be a modulation product $2\omega_1 - \omega_f$ close to the fundamental.

The slope of the lines is 2 which means that the frequency shift of the fundamental is proportional to the square of the input disturbance. Further, the spacing between the lines indicates that:

$$\text{Frequency Shift} \quad \propto \quad \frac{1}{(\frac{\omega_1}{\omega_o} - 1)^3}$$

In addition to the curves of Figure 4.7, Figure 4.8 also shows curves for driving frequencies less than the fundamental. In this case, the frequency shift is negative (i.e. the shift is still towards the driving frequency) and so these curves have been shown dashed.

The dependence of the shift on $\alpha$, the small parameter describing the "degree" of nonlinearity in equation (1) was found difficult to determine and no significant results were obtained, although there were indications that a square relation may hold.

Empirically, therefore, the approximate relation

$$\text{Frequency Shift} \quad \propto \quad \frac{I^2}{(\frac{\omega_1}{\omega_o} - 1)^3}$$

was found to hold for the experimental oscillator.

The same dependence also holds true if narrow band noise is used as an input, the portions of the curves of Figure 4.6 below the "knee" being similar to the curves of Figure 4.7.

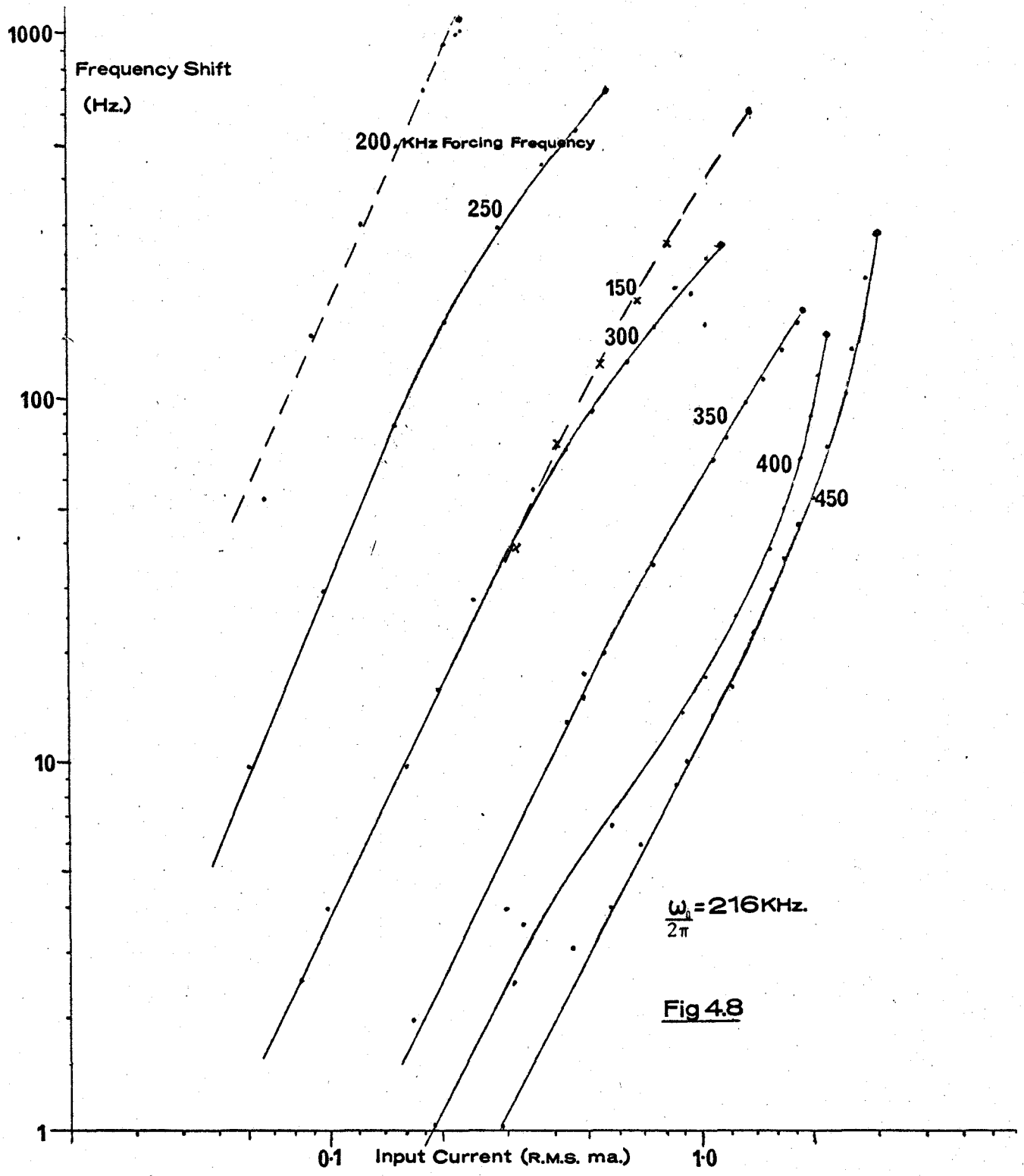


Fig 4.8

Frequency Shift vs. Input Current (Sinusoidal Input).

4.8 Accuracy:

The oscillator was found to be stable (after a warm-up period of several days) to 3 parts in $10^7$ over a period of one minute. It was thus possible to detect frequency shifts as low as .5 Hz, or about 3 parts in $10^7$ with an accuracy of the order of 10% (determined by the "repeatability" of the measurements). At higher inputs and hence larger frequency shifts, the error is proportionately smaller.

The accuracy of measurement of a, the nonlinear parameter was considered good (2%). The value of b (obtained from a and the free running amplitude) is therefore of a similar accuracy. The presence of an element of nonlinear capacitance in the circuit was found very difficult to investigate; an analysis of the circuit was attempted, to investigate the effect of the grid-cathode capacitance on the nonlinear resistance, but it was found that this led to expressions far too unwieldy to be of any practical assistance. The presence of a small nonlinear reactance cannot be discounted, and this may account for the difference between the measured and calculated values, in addition to the experimental errors mentioned above.

Thus, although the accuracy of the measurement of the frequency shift was acceptable, there were additional uncertainties caused by the above, which although negligible in the first order, become significant when second order effects such as frequency deviation are considered. Hence although qualitative conclusions can be drawn, accurate quantitative conclusions would require a much more sophisticated experimental investigation to eliminate any spurious nonlinearities, in particular nonlinear reactance, or any slight

assymmetry of the nonlinear characteristics which would introduce even harmonics at the output. These will tend to lower the free running frequency[16]. Also, second harmonic resonances may occur which probably account for the shape of the second and half harmonic curves of figures (4.5, 4.6, 4.7). However, the square and quintic terms in the nonlinearity were very small, and would only assume importance near the second and fifth harmonics. A more detailed analysis would be required to ascertain the effect of these additional terms.

# CHAPTER V

# CONCLUSIONS

The frequency shift of the van der Pol oscillator due to an external forcing sinusoid has been experimentally found to be proportional to

$$\Delta f \propto \frac{I^2}{(a-1)^3}$$

where I is the input current magnitude and a is the ratio of the forcing frequency to the free frequency. This is in agreement with the calculated shift (equation (34)):

$$\Delta f = \omega_o \frac{\alpha^2}{4} \left(\frac{I}{\omega_o C}\right) \frac{a^2 (2-a)(1+(2-a)^2)}{(a-1)^3(1+a)^2(3-a)^2} \qquad (34)$$

Unfortunately, the experimental data was not accurate enough to observe the effect of the other poles and zeros of equation (34).

The result of A. W. Gillies[12a] showed that the frequency shift was proportional to the square of the input, but did not give as good results as equation (34) for the magnitude of the shift.

The maximum frequency shift occurred just before synchronization, and was calculated to be (equation (26))

$$\Delta f = \frac{\alpha^2}{16} \frac{\omega_1^2}{(\omega_1^2 - 1)} \qquad (26)$$

Equations(34) and (26) are both in good qualitative agreement with the experiment, but are only fair quantitatively.

## APPENDIX A

## THE METHOD OF VAN DER POL

The van der Pol equation was first solved by Balthazar van der Pol after whom the equation is named[1]. In this Appendix, his method of solution is presented, and an expression for the magnitude of the input signal for the oscillator to just be synchronized is derived. The driven van der Pol equation (Equation (2)) is

$$\ddot{e} - \alpha(1 - \beta e^2)\,\omega_o \dot{e} + \omega_o{}^2 e = \left(-\frac{I}{C}\right)\,\omega_1 \sin \omega_1 t$$

where

$$\alpha = \frac{a}{C\omega_o} \qquad \beta = \frac{3b}{a} \qquad \omega_o{}^2 = \frac{1}{LC} \tag{A1}$$

and a, b are the nonlinear element parameters.

L, C are the antiresonant circuit elements in Figure 2.1.

Assume a general solution of the form

$$e = b_1 \sin \omega_1 t + b_2 \cos \omega_1 t \tag{A2}$$

where the possible presence of a free oscillation is allowed for by letting $b_1$ and $b_2$ be slowly varying functions of time (varying slowly enough so that $\ddot{b}_1$ and $\ddot{b}_2$ can be neglected, where the dot represents differentiation with respect to time, and $\dot{b_1} << \omega_1 b_1$, $\dot{b_2} << \omega_1 b_2$).

If Equation (A2) is substituted into Equation (A1), and coefficients of sin $\omega_1 t$ and cos $\omega_1 t$ equated, the following two equations are obtained.

$$2\dot{b_1} + \alpha\omega_o x\, b_2 - \alpha b_1\left(1 - \frac{\beta}{4} b^2\right)\omega_o = 0 \qquad (A3a)$$

$$2\dot{b_2} - \alpha\omega_o x\, b_1 - \alpha b_2\left(1 - \frac{\beta}{4} b^2\right)\omega_o = \left(-\frac{I}{C}\right) \qquad (A3b)$$

where $$x = \frac{\omega_o^2 - \omega_1^2}{\alpha\omega_1\omega_o}, \quad b^2 = b_1^2 + b_2^2$$

and $\frac{2}{\sqrt{\beta}}$ = free running amplitude.

A particular solution of equations (A3) is given by:

$$\dot{b_1} = \dot{b_2} = 0$$

and hence,

$$\alpha x b_2 - \alpha b_1\left(1 - \frac{\beta}{4} b^2\right) = 0 \qquad (A4a)$$

$$\alpha x b_1 + \alpha b_2\left(1 - \frac{\beta}{4} b^2\right) = \frac{I}{C\omega_o} \qquad (A4b)$$

Squaring and adding equations (A4) gives:

$$b^2\left[x^2 + \left(1 - \frac{\beta}{4} b^2\right)^2\right] = \left(\frac{I}{\alpha\omega_o C}\right) \qquad (A5)$$

or

$$y\left[x^2 + (1 - y)^2\right] = E^2 \qquad (A6)$$

where $y = \frac{\beta b^2}{4}$ and $E^2 = \frac{\beta}{4}\left(\frac{I}{\alpha\omega_o C}\right)^2$

These are the resonance curves for the van der Pol oscillator, and are shown in Figure A1 , where x is proportional to the frequency difference $\omega_o^2 - \omega_1^2$, or the "detuning" of the input, and y is proportional to the magnitude squared of the resultant oscillator output. Since, for this solution, $\dot{b_1} = \dot{b_2} = 0$, Equation (A5) must represent the oscillator in the synchronized state with the free oscillation suppressed.

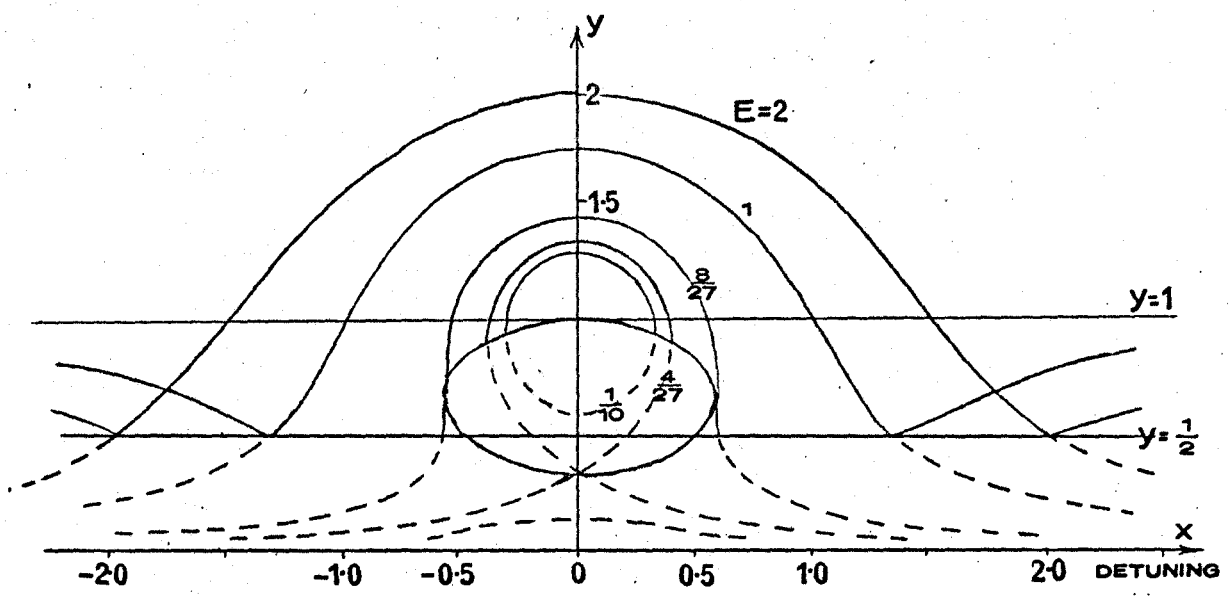


FIGURE (A1): Resonance Curves for the van der Pol Oscillator

The stability of the system can be investigated by examining the behaviour of small variations in $b_1$ and $b_2$ with respect to time. This may be accomplished by substituting $b_1 + \Delta b_1$ and $b_2 + \Delta b_2$ for $b_1$ and $b_2$ in Equations (A3), to form another pair of equations. Equations (A3) are then subtracted from these new equations, which are then solved for $\Delta b_1$ or $\Delta b_2$. The resulting linear equation is:

$$4\Delta\ddot{b}_1 - 4\alpha\omega_o\Delta\dot{b}_1(1 - \frac{\beta}{2}b^2) + \Delta b_1\alpha^2\omega_o{}^2\left[(1 - \frac{\beta}{4}b^2)(1 - \frac{3}{4}\beta b^2) + x^2\right] = 0$$

The Routh stability criteria gives the conditions:

$$-4\alpha\ (1 - \frac{\beta}{2}b^2) > 0$$

$$\alpha^2\left[(1 - \frac{\beta}{4}b^2)(1 - 3\frac{\beta}{4}b^2) + x^2\right] > 0$$

which can be rewritten,

$$y > \frac{1}{2} \qquad \text{(A7)}$$

$$x^2 + (1 - y)(1 - 3y) > 0 \qquad \text{(A8)}$$

Equation (A8) is the ellipse shown in Figure (A1).

The synchronization range for large input amplitudes and detuning is governed by equation (A6), and by the boundary condition (A7). Hence, on the stability boundary,

$$E^2 = \frac{1}{2}\left[x^2 + \frac{1}{4}\right]$$

That is,

$$\frac{I^2\beta}{4\alpha^2\omega_o{}^2C^2} = \frac{1}{2}\left[\frac{(\omega_o{}^2 - \omega_1{}^2)^2}{\alpha^2\omega_1{}^2\omega_o{}^2} + \frac{1}{4}\right]$$

and hence,

$$I^2 = \frac{2C^2}{\beta}\left[\frac{(\omega_o{}^2 - \omega_1{}^2)^2}{\omega_1{}^2} + \frac{\alpha^2\omega_o{}^2}{4}\right] \qquad \text{(A9)}$$

which is plotted, for the oscillator experimentally measured, in Figure A2. Some experimental points are also plotted, showing good agreement.

If $\omega_o \doteqdot \omega_1$ and the term in $\alpha^2$ is negligible,

$$I \doteqdot \sqrt{\frac{2}{\beta}} \quad 2C\ [\omega_o - \omega_1]$$

where C is the tank circuit capacitance and $2/\sqrt{\beta}$ is the free running amplitude.

That $b_1$ and $b_2$ are slowly varying (particularly when $\omega_o - \omega_1$ is small) can be seen experimentally from the waveforms in Figure (4A).

The solution,

$$e = b_1 \sin \omega t + b_2 \sin \omega_1 t \qquad \text{(A10)}$$

could have been used instead of equation (A2). This form is more convenient for examining the response when both free and forced oscillations are present[1,2]. In this case, the resonance curves are,

$$y\ [x^2 + (1 - 3y^2)^2] = E^2 \qquad \text{(A11)}$$

where

$$y = \frac{\beta}{4} b_2^2$$

and the amplitude of the free oscillation is given by:

$$b_1^2 = \frac{4}{\beta} - 2b_2^2 \qquad \text{(A12)}$$

The connection between curves (A6) and curves (A11) is good away from the ellipse but is incomplete in a small region about the ellipse. A more accurate solution of equation (A1) is required to complete the curves.

Fig. A2

Locking Current vs Frequency for the van der Pol Oscillator

— Calculated Curve

0 Experimental Points

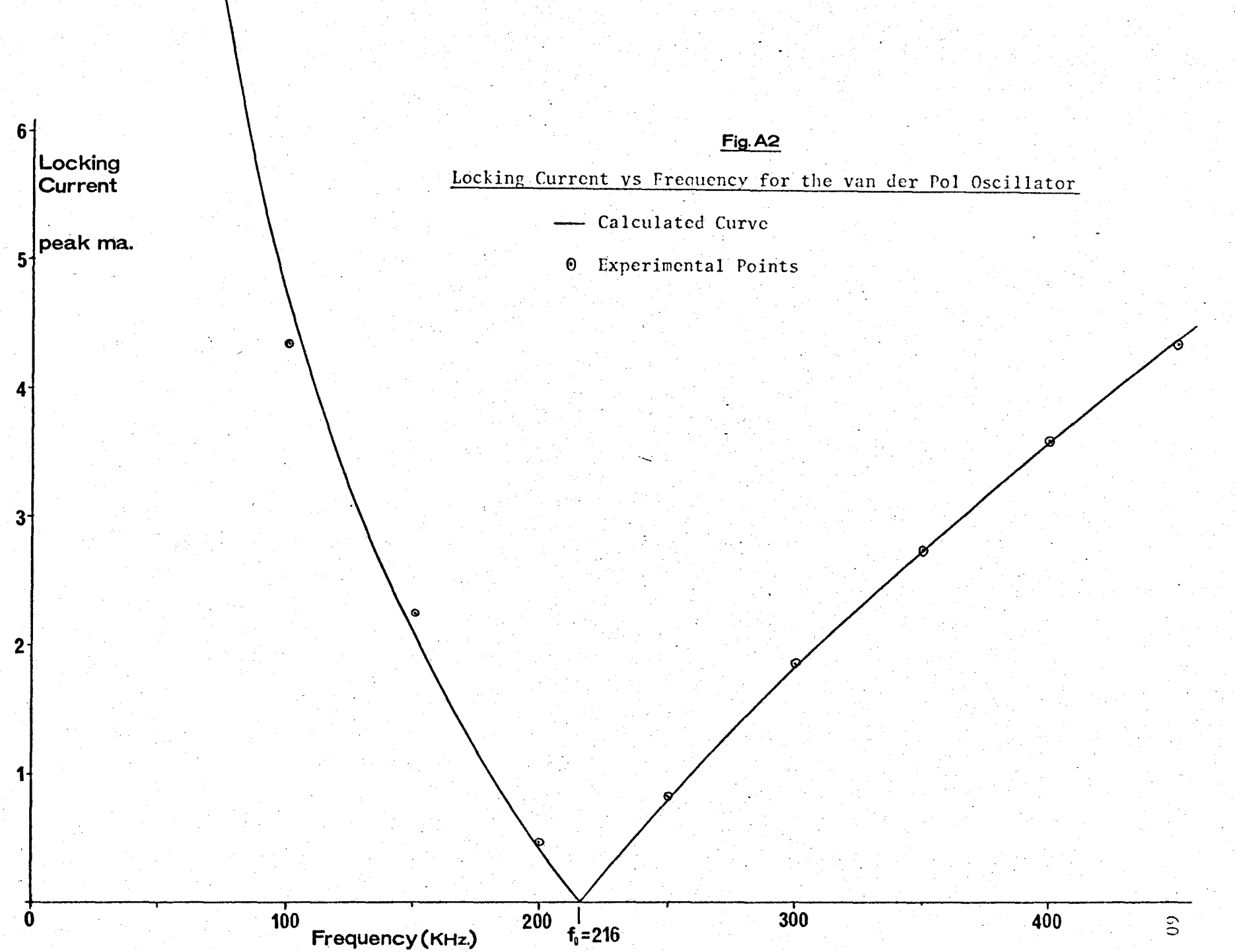

# APPENDIX B

## FREQUENCY COMPARISON

The following method[23] may be used to identify the harmonics in the oscillator output and obtain a qualitative estimate of their magnitudes.

The system is shown in Figure B1, below.

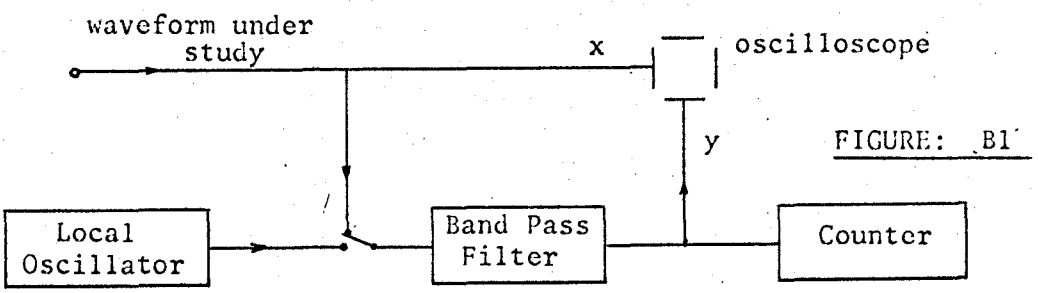


FIGURE: B1

The waveform to be studied is applied directly to the x plates of an oscilloscope, and through a variable narrow-bandpass filter to the y plates. The input to the x plates can be considered as $\sum_{i=1}^{\infty}$ sin $n_i\omega t$ and that to the y plates as sin $n_i\omega t$ if the filter is turned to the $i^{th}$ frequency component. An ellipse will appear on the screen, and if this frequency is unrelated to any other x plate frequency, this ellipse will move in a stationary envelope (e.g. if $x = \sin \omega_o t + \sin \omega_1 t$ and $y = \sin \omega_1 t$, then an ellipse of frequency $\omega_1$, moving horizontally with a frequency $\omega_o$ will appear as in Figure B2 ).

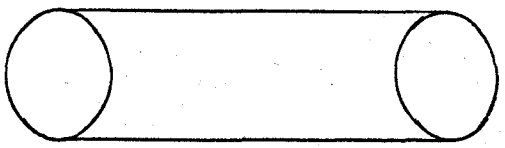

FIGURE B2

In this way, by tuning the filter correctly, the sidebands may be isolated, and an approximate value of their magnitudes obtained by measuring the size of the ellipses.

This method was found to be more convenient than beating the unknown x waveform with a local oscillator. Due to random frequency drifts of both, it was found difficult to stabilize the display. As the filter output was small (particularly for the smaller sidebands), a local oscillator could be substituted and tuned to the filter frequency, in order to measure frequencies more accurately, as shown in Figure B1.

## APPENDIX C

## COMPUTER ANALYSIS

The van der Pol equation was solved on a digital computer to give the oscillator output under different conditions.

The analogue-digital simulators MIMIC and MIDAS were used. By means of these preprocessing routines it is possible to run an analogue computer programme on a digital computer. There are several advantages in doing this; greatly increased accuracy; no time or magnitude scaling problems; 95 integrators (MIMIC), or 100 (MIDAS) are available, and any number of summing amplifiers, function generators, etc. is permitted. Both processors have the built in facility of automatically selecting a step size for the numerical integration routine to maintain a given accuracy. MIMIC has a limited capability for hybrid computation by means of the Track And Store (TAS) subroutine, although trouble has been experienced with this if more than two parameters need to be recalculated.

Of the two processors, MIMIC is easier to programme, it being possible to write the programme directly from the system differential equation. MIDAS requires a block diagram to be prepared initially. Of the two, MIMIC is the faster, the execution times for the MIMIC and MIDAS programmes, 1 and 2 given below, being 100 seconds and 240 seconds respectively. MIDAS is, however, the easier of the two systems for "debugging" programme errors, and the processor also prints out the maxima and minima of all the system variables, unlike MIMIC.

The programmes which solve the van der Pol equation are given in the following pages. Programme 1 is a MIMIC source language programme, and programme 2 is in MIDAS language. Both solve the system for the initial build up of oscillations when the oscillator is switched on. The output from these programmes is shown in Figure (C1). A forcing term F(t) can be inserted in the programmes, and Figure (C2) shows the computed output for a forcing current of 0.5 mA at 250KHz. This can be compared with Figure 4.4 which shows the waveform of the experimental oscillator under similar conditions.

Using MIMIC, 200 points of a cycle of the steady free running oscillator were computed. These were analyzed by a Fourier Analysis programme (programme 3) and the results of this are given with the programme. They are in excellent agreement with the solution calculated in Chapter 2.

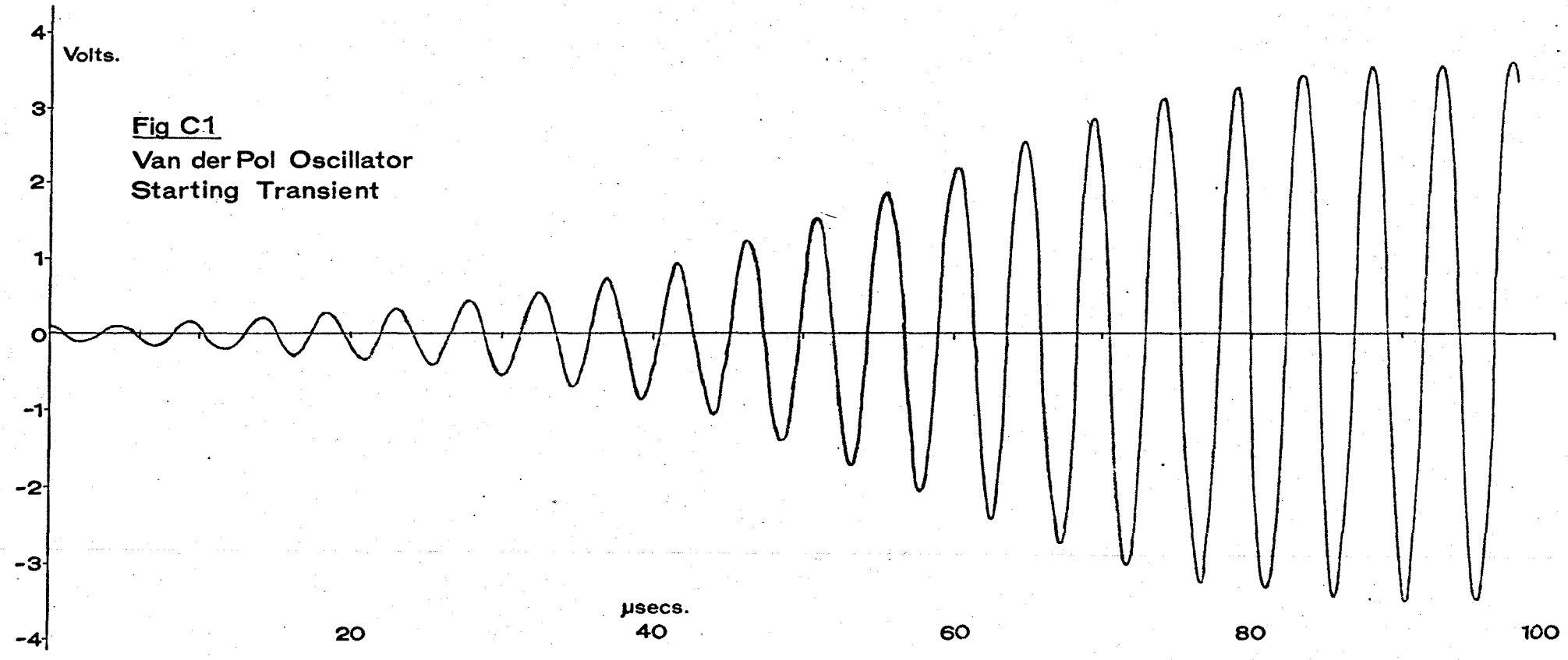


Fig C1
Van der Pol Oscillator
Starting Transient

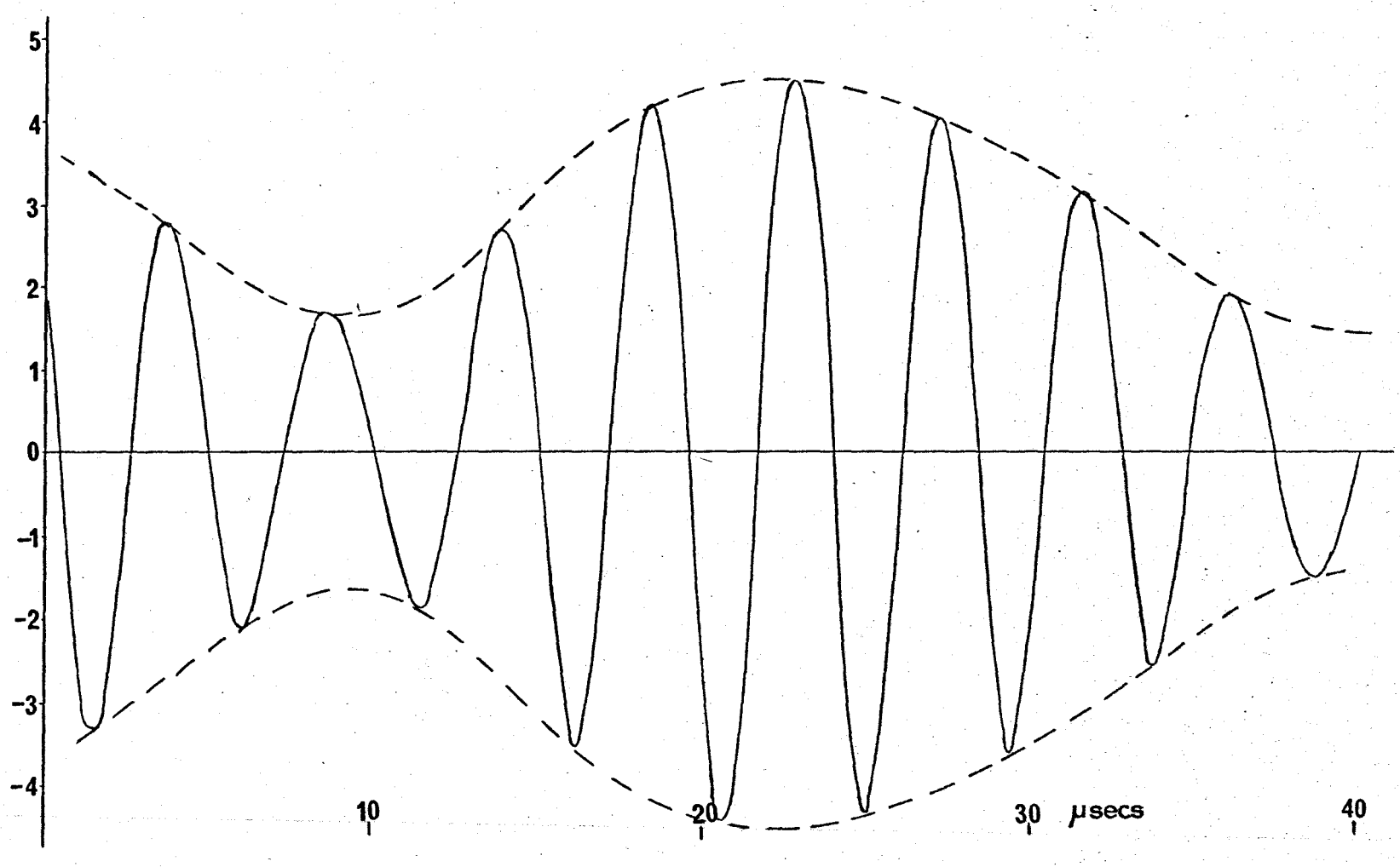


FIGURE (C2): The Forced van der Pol Oscillator

Forcing Current = 0.5 Peak ma at 250 KHz (MIMIC Solution)

PROGRAMME 1  MIMIC SOLUTION.

```
$EXECUTE        MIMIC
                   CON(AL,BT,W0,DT)
          D2X      ADD(AL*(1.0-BT*X*X)*W0*D1X,-W0*W0*X)
          D1X      INT(D2X,0.0000)
          X        INT(D1X,0.1    )
                   FIN(T,150.0)
                   OUT(T,X,D1X)
                   HDR(T,X,D1X)
                   HDR
                   END
0.0819       0.2973        1.357         0.2
```

PROGRAMME 2  MIDAS SOLUTION.

```
OSCILLATOR CONSTANTS
      CON      AL,BT,W0,TR,TF,1.          W0 NOT NORMALIZED
INITIAL CONDITIONS
      IC       I1,I2                   GIVES STARTING TRANSIENT
PATCH BOARD CONNECTIONS
      I1       S2              EDOT
      I2       I1              E
      M1       I2,I2           ) NONLINEAR
      M2       M1,BT           ) TERM
      S1       M2,1.
      M5       AL,W0
      M3       S1,M5
      M4       M3,I1
      M7       W0,W0
      M6       M7,I2
      NEG1     M6
      S2       M4,NEG1         EDOUBLEDOT
      FIN      IT,TF
      HDR      TIME,E,EDOT
      HDR
      RO       IT,I2,I1        WHERE IT=TIME
      END           CONSTANTS AND INITIAL CONDITIONS FOLLOW
.0819     -.2973     1.357      .2          150.       1.
0.         0.1
```

PROGRAMME 3 FOURIER ANALYSIS.

```
$IBFTC MAIN
C FOURIER ANALYSIS OF 'FREE RUNNING VAN DER POL OSCILLATOR.
      DIMENSION B(200), C(12), S(12), V(12), ANG(12)
      READ(5,1) B
      M=12
      N=200
      WRITE(6,3) B
      CALL FORAN(B,N,M,C,S,V,ANG,AAVG)
      WRITE(6,2) AAVG
      DO 20 J=1,M
    4 FORMAT(3H C(,I2,4H) = ,E14.8,8H      S(,I2,4H) = ,E14.8,5X,2HV(,I2
     1,4H) = ,E14.8,5X,4HANG(,I2,4H) = ,F8.3,4HDEGS)
    2 FORMAT(/9H C( 0) = ,E14.8)
      WRITE(6,4)   J, C(J), J, S(J), J, V(J), J, ANG(J)
   20 CONTINUE
    1 FORMAT(8F10.6)
    2 FORMAT( 7H C( 0)=  ,E11.5 )
    3 FORMAT(1X,8F14.6)
    4 FORMAT(3H C(,I2,2H)=  ,E11.5,3X,   2HS(,I2,2H)=  ,E11.5,3X,2HV(,I2
     1,2H)=  ,E11.5,3X,4HANG(,I2,2H)=  ,F6.1,4HDEGS)
      STOP
      END
$ENTRY
$IBSYS
```

```
$IBFTC FORAN
C N-POINT FOURIER ANALYSIS
C  POINTS EQUALLY SPACED OVER ONE PERIOD.  THE LAST (2PI) POINT IS THE
C  N+1TH POINT AND IS NOT USED.
C N=NUMBER OF POINTS
C M=NUMBER OF HARMONICS REQUIRED
C ANSWERS ARE--
C C=ARRAY OF COSINE TERMS
C S=ARRAY OF SINE TERMS
C V=ARRAY OF VECTORS
C ANG=ARRAY OF VECTOR ANGLES
C AAVG=D.C. COMPONENT
      SUBROUTINE FORAN(B,N,M,C,S,V,ANG,AAVG)
      DIMENSION B(N),C(M),S(M),V(M),ANG(M)
      MM=M
      IF(N.GE.2*M) GO TO 200
      MM=N/2
      WRITE(6,198) MM
  198 FORMAT(1H0, 20HONLY ENOUGH DATA FOR , I3, 12H HARMONICS. ,
     1 29HHIGHER HARMONICS SET TO ZERO. /)
      K=MM+1
      DO 199 I=K,M
      C(I)=0.
      S(I)=0.
      V(I)=0.
      ANG(I)=0.
  199 CONTINUE
  200 CONTINUE
      ZN=N
      AAVG=0.0
      DO 201 I=1,N
  201 AAVG=AAVG+B(I)
      AAVG=AAVG/ZN
      DO 205 J=1,MM
      ZJ=J
      C(J)=0.
      S(J)=0.
      AL=6.2831853*ZJ/ZN
      DO 202 I=1,N
      A1=I-1
      S(J)=S(J)+SIN(AL*A1)*B(I)
      C(J)=C(J)+COS(AL*A1)*B(I)
  202 CONTINUE
      IF(J.NE.N/2) GO TO 203
      C(J)=C(J)/2.0
      S(J)=S(J)/2.0
  203 CONTINUE
      S(J)=S(J)*2.0/ZN
      C(J)=C(J)*2.0/ZN
      V2=C(J)*C(J)+S(J)*S(J)
      V(J)=SQRT(V2)
      ANG(J)=ATAN2(C(J),S(J))
      ANG(J)=ANG(J)*57.29578
  205 CONTINUE
      RETURN
      END
```

```
-0.0033    .112157    .227799    .343509    .459166    .574649    .689832    .804587
.918786    1.03230    1.14499    1.25672    1.36737    1.47679    1.58485    1.69141
1.79634    1.89951    2.00079    2.10004    2.19714    2.29196    2.38438    2.47428
2.56155    2.64609    2.72777    2.80652    2.88222    2.95480    3.02417    3.09025
3.15297    3.21228    3.26810    3.32039    3.36911    3.41422    3.45567    3.49346
3.52755    3.55793    3.58459    3.60754    3.62676    3.64228    3.65409    3.66222
3.66668    3.66750    3.66470    3.65832    3.64839    3.63494    3.61802    3.59767
3.57392    3.54682    3.51643    3.48278    3.44592    3.40592    3.36281    3.31665
3.26749    3.21539    3.16040    3.10257    3.04197    2.97863    2.91263    2.84401
2.77284    2.69917    2.62306    2.54456    2.46374    2.38065    2.29537    2.20794
2.11843    2.02691    1.93344    1.83808    1.74092    1.64200    1.54142    1.43923
1.33553    1.23037    1.12385    1.01605    .907056    .796950    .685826    .573777
.460901    .347297    .233067    .118317    .003156   -.112305   -.227951   -.343665
-.459327   -.574814   -.690000   -.804759   -.918960  -1.03247   -1.14517   -1.25690
-1.36755   -1.47697   -1.58503   -1.69160   -1.79654   -1.89971   -2.00098   -2.10024
-2.19733   -2.29215   -2.38457   -2.47448   -2.56175   -2.64628   -2.72797   -2.80671
-2.88241   -2.95499   -3.02435   -3.09043   -3.15315   -3.21246   -3.26828   -3.32057
-3.36928   -3.41438   -3.45583   -3.49361   -3.52770   -3.55808   -3.58474   -3.60768
-3.62690   -3.64241   -3.65422   -3.66234   -3.66679   -3.66761   -3.66481   -3.65842
-3.64849   -3.63504   -3.61811   -3.59775   -3.57399   -3.54689   -3.51649   -3.48284
-3.44598   -3.40597   -3.36285   -3.31669   -3.26752   -3.21542   -3.16042   -3.10259
-3.04198   -2.97864   -2.91263   -2.84401   -2.77283   -2.69915   -2.62303   -2.54453
-2.46371   -2.38062   -2.29532   -2.20789   -2.11838   -2.02685   -1.93338   -1.83802
-1.74084   -1.64193   -1.54134   -1.43915   -1.33543   -1.23028   -1.12375   -1.01595
-.906946   -.796836   -.685707   -.573655   -.460775   -.347166   -.232932   -.118179

C( 0)=-0.3775E-04
C( 1)= 0.3434E-01   S( 1)= 0.3668E 01   V( 1)= 0.3668E 01   ANG( 1)=   0.5DEGS
C( 2)= 0.2072E-04   S( 2)=-0.6490E-04   V( 2)= 0.6813E-04   ANG( 2)= 162.3DEGS
C( 3)=-0.3745E-01   S( 3)= 0.2170E-02   V( 3)= 0.3752E-01   ANG( 3)= -86.7DEGS
C( 4)= 0.4875E-05   S( 4)=-0.2367E-04   V( 4)= 0.2417E-04   ANG( 4)= 168.4DEGS
C( 5)=-0.6482E-04   S( 5)=-0.6549E-03   V( 5)= 0.6581E-03   ANG( 5)=-174.3DEGS
C( 6)= 0.8788E-06   S( 6)=-0.1500E-04   V( 6)= 0.1503E-04   ANG( 6)= 176.6DEGS
C( 7)= 0.1231E-04   S( 7)=-0.1516E-04   V( 7)= 0.1952E-04   ANG( 7)= 140.9DEGS
C( 8)=-0.1362E-06   S( 8)=-0.1142E-04   V( 8)= 0.1142E-04   ANG( 8)=-179.3DEGS
C( 9)=-0.5257E-06   S( 9)=-0.1008E-04   V( 9)= 0.1009E-04   ANG( 9)=-177.0DEGS
C(10)=-0.5112E-06   S(10)=-0.9412E-05   V(10)= 0.9426E-05   ANG(10)=-176.9DEGS
C(11)=-0.9466E-06   S(11)=-0.8275E-05   V(11)= 0.8329E-05   ANG(11)=-173.5DEGS
C(12)=-0.1228E-05   S(12)=-0.7891E-05   V(12)= 0.7986E-05   ANG(12)=-171.2DEGS

**********
```

# APPENDIX D

## APPARATUS

Power Supply, John Fluke moder 407

Oscillator, Hewlett Packard moder 241A

Cathode Follower Probes and Power Supply, Type 128, Tektronix

Oscilloscopes, Tektronix Types 502A and 516

Counters, Beckman model 7370, Hewlett Packard model 5245L

Random Noise Generator, General Radio Company, Type 1390B

V.T.V.M., John Fluke, model 910A

REFERENCES


1. van der Pol, B., "Forced Oscillations in a Circuit with Nonlinear Resistance", Phil. Mag. Vol. 3, No. 13, p. 65, 1927.
2. Cunningham, W. J., "Introduction to Nonlinear Analysis", McGraw-Hill Book Co., Inc., 1958.
3. Hayashi, C., "Oscillation in Nonlinear Systems", McGraw-Hill Book Company, 1965.
4. Stoker, J. J. "Nonlinear Vibrations", Interscience Pub. Inc., N.Y. 1950.
5. Stern, T. E., "Theory of Nonlinear Networks and Systems", Addison-Wesley Pub., 1965.
6. Kuznetsov, P. I., Stratonovich, R. L., Tikhonov, V. I., "Nonlinear Transformations of Stochastic Processes", Ch. III, Pergamon Press 1965.
7. Edson, W. A., "Noise in Oscillators", Proc. IRE, Vol. 8, p. 1454 August, 1960.
8. Mullen, J. A.,"Background Noise in Nonlinear Oscillators", Proc IRE Vol. 48, p. 1467, August, 1960.
9. Golay, J. E., "Monochromacity and Noise in a Regenerative Electrical Oscillator", Proc. IRE, Vol. 48, P. 1473, August, 1960. and, "Normalized Equations of the Regenerative Oscillator-Noise, Phase Locking and Pulling", Proc. IRE, Vol. 52, p. 1311, November 1964.

10a. Rytov S.M.,"Fluctuations in Oscillating Systems of the Thomson Type,I and II", Soviet Phys. JETP, Vol. 2, p.217, March 1956.

10b. Tang, C. L. "The Behaviour of Nonlinear Oscillating Systems in the Presence of Noise", Proc. IEEE, Vol. 48, p. 1493, August, 1960.

11a. Hafner, E., "The Effects of Noise on Oscillators", Proc. IEEE, Vol. 54, No. 2, February 1966.

11b. Mullen, J. A., Hafner, E., "Comments on the Effects of Noise in Oscillators", Proc. IEEE, Vol 55, No. 1, p. 87, January 1967.

12a. Gillies, A. W., "The Application of Power Series to the Solution of Non-Linear Circuit Problems", Proc. IEE, Vol. 96 III No. 44 November, 1949.

12b. Gillies, A. W., "Electrical Oscillations - A Physical Approach to the Phenomena", Wireless Engineer, Vol. 30, No. 6, June, 1953.

13. Raue, G. E., Ishii, T. K., "Analysis of Observed Spectrum in the Pulling of Millimeter Reflex Klystrons", Proc. IEEE, Vol. 54, No.12 p. 1942, December, 1966.

14. Groszkowski, J., "The Interdependence of Frequency Variation and harmonic Content and the Problem of Constant Frequency Oscillators", Proc. IRE, Vol. 21, pp. 958-981, May 1933.

15. Yogev, M., "Noise in Oscillators - Experimental Results", Proc. IEEE, Vol. 51, p. 1681, 1963.

16. Gladwin, A. S., "The Frequency of a Nonlinear Oscillator with a Perturbing Force", Proc. IEEE, Vol. 55, No. 2, p. 246, Feb. 1967.

17. Garstens, M. A., "Noise in Nonlinear Oscillators", J. App. Phys. Vol. 28, No. 1, p. 352, March 1957.

18. Mullen, J. A., "Background Noise in Nonlinear Oscillators", Proc. IEEE, Vol. 48, p. 1467, August 1960.

19. Golay, M. J., "Monochromacity in a Regenerative Electrical Oscillator", Proc. IEEE, Vol. 48, p. 1473, August 1960.

20. Adler, R., "A Study of Locking Phenomena in Oscillators", Proc. IEEE, Vol. 34, p. 351, June 1946.

21. Stover, H. L., "Theoretical Explanation for the Output Spectra of Unlocked Driven Oscillators", Proc. IEEE, Vol 54, No. 2, p. 310 February 1966.

22. Davenport and Root, "Random Signals and Noise", McGraw-Hill, 1958.

23. Jones, N. B.,"The Generation of Simultaneous Oscillations at Unrelated Frequencies using a single Non-Linear Element", Thesis, McMaster University, 1965.

24. Ponzo, P. J., Way, N., "On the Periodic Solution of the van der Pol Equation", Proc. IEEE, CT-12 pp. 135-6, March 1965.

25. Hakki, B., Beccone, J. P. and Plauski, S. E., "Phase-Locked GaAs Microwave Oscillators", Proc. IEEE, ED-13, pp. 197-199, Jan. 1966.

---------oOo---------